Multi-band optical imaging

From fusion to change detection

Nicolas Dobigeon

Joint work with Q. Wei, V. Ferraris, J.-Y. Tourneret and M. Chabert

University of Toulouse, IRIT/INP-ENSEEIHT
Institut Universitaire de France (IUF)
Artificial and Natural Intelligence Toulouse Institute (ANITI)
`http://dobigeon.perso.enseeiht.fr`

ORASIS 2021, Lac de St-Ferréol

Multi-band optical imaging

Multi/hyper-spectral images

- same scene observed at different wavelengths

Multi-band optical imaging

Multi/hyper-spectral images

- same scene observed at different wavelengths

Hyperspectral Cube

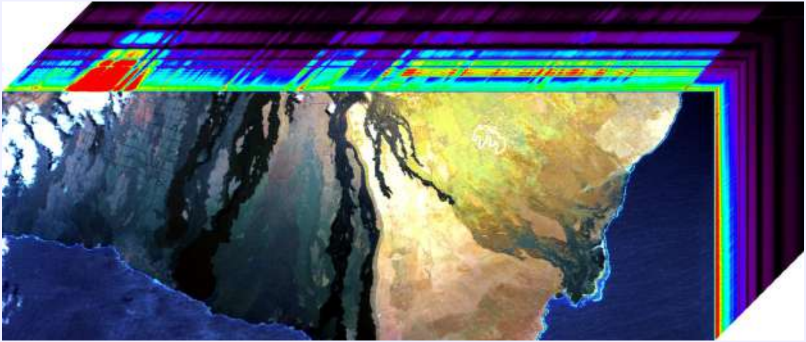

Multi-band optical imaging

Multi/hyper-spectral images

- same scene observed at different wavelengths,
- pixel represented by a vector of tens/hundreds of measurements.

Multi-band optical imaging

Multi/hyper-spectral images

- same scene observed at different wavelengths,
- pixel represented by a vector of tens/hundreds of measurements.

Hyperspectral Cube

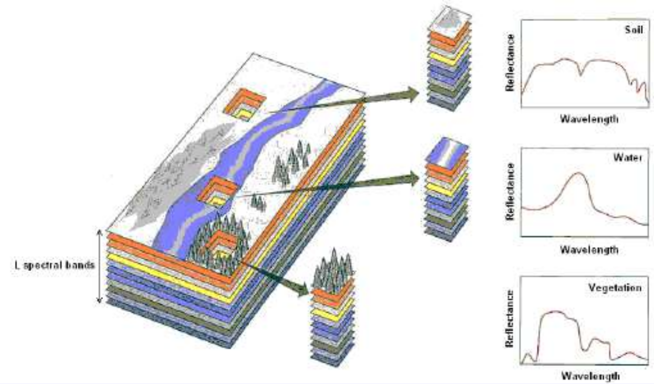

Multi-band optical imaging

Multi-band optical imaging

Multi-band optical imaging

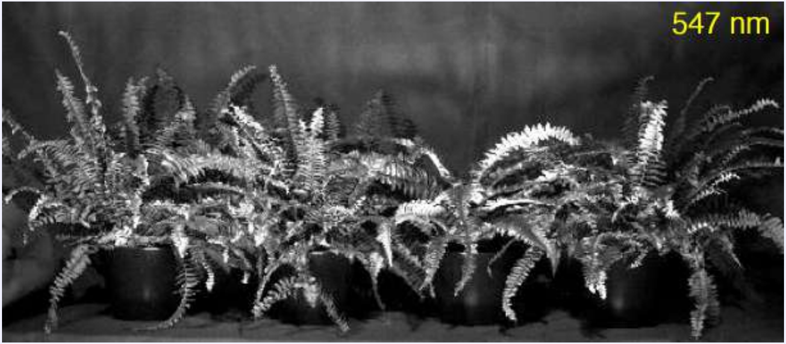

Multi-band optical imaging

Multi-band optical imaging

Multi-band optical imaging

Multi-band optical imaging

Spatial vs. spectral resolution trade-off

Panchromatic images (PAN)

- no spectral resolution (only 1 band),
- very high spatial resolution ($\sim$ 10cm).

Multispectral images (MS)

- low spectral resolution ($\sim$ 10 bands),
- high spatial resolution ($\sim$ 1m).

Hyperspectral images (HS)

- high spectral resolution ($\sim$ 100 bands),
- low spatial resolution ($\sim$ 10m).

Multi-band optical imaging
Spatial vs. spectral resolution trade-off

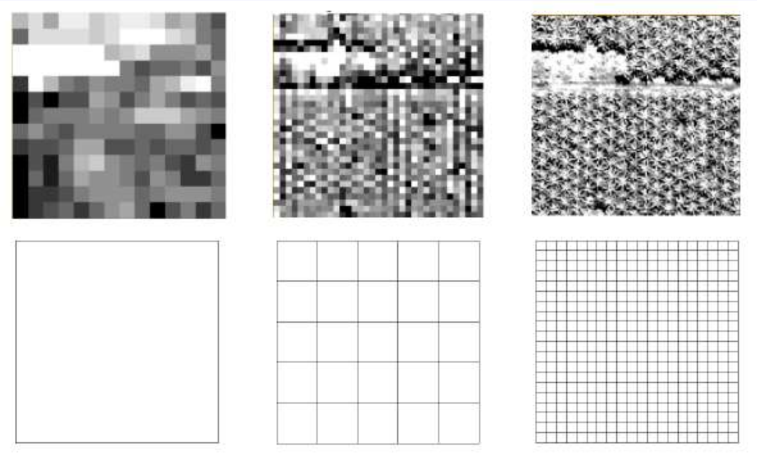

Spot HS (20m) Quickbird MS (4m) Ikonos PAN (1m)

Outline

Introduction

Multi-band optical image fusion
- Problem statement
- Fast fusion solving a Sylvester equation
- Experiments

Multi-band optical image change detection
- Fusion approach
- Robust Fusion approach

Conclusions

Outline

Introduction

Multi-band optical image fusion
- Problem statement
- Fast fusion solving a Sylvester equation
  - From maximum likelihood estimator...
  - ... to maximum a posteriori estimators
- Experiments

Multi-band optical image change detection
- Fusion approach
- Robust Fusion approach

Conclusions

Multiple image fusion

Pansharpening: PAN+MS fusion

- incorporate the spatial details of the PAN image into the MS image
- huge literature
- main approaches rely on band substitution

Hyperspectral pansharpening: PAN+HS fusion

- incorporate the spatial details of the PAN image into the HS image
- more difficult due to the size of the HS image
- specific methods should be developed

Multi-band image fusion: MS+HS fusion

- incorporate the spatial details of the MS image into the HS image
- more difficult since the spatial details contained in a multi-band image
- specific methods should be developed

Multiple image fusion

Pansharpening: PAN+MS fusion

- incorporate the spatial details of the PAN image into the MS image
- huge literature
- main approaches rely on band substitution

Hyperspectral pansharpening: PAN+HS fusion

- incorporate the spatial details of the PAN image into the HS image
- more difficult due to the size of the HS image
- specific methods should be developed

Multi-band image fusion: MS+HS fusion

- incorporate the spatial details of the MS image into the HS image
- more difficult since the spatial details contained in a multi-band image
- specific methods should be developed

Multiple image fusion

Pansharpening: PAN+MS fusion

- incorporate the spatial details of the PAN image into the MS image
- huge literature
- main approaches rely on band substitution

Hyperspectral pansharpening: PAN+HS fusion

- incorporate the spatial details of the PAN image into the HS image
- more difficult due to the size of the HS image
- specific methods should be developed

Multi-band image fusion: MS+HS fusion

- incorporate the spatial details of the MS image into the HS image
- more difficult since the spatial details contained in a multi-band image
- specific methods should be developed

Multiple image fusion

Hyperspectral pansharpening: PAN+HS fusion

- incorporate the spatial details of the PAN image into the HS image
- more difficult due to the size of the HS image
- specific methods should be developed

Multi-band image fusion: MS+HS fusion

- incorporate the spatial details of the MS image into the HS image
- more difficult since the spatial details contained in a multi-band image
- specific methods should be developed

Problem statement

(a) Hyperspectral Image (size: 99 $\times$ 46 $\times$ 224, res.: 20m $\times$ 20m) (b) Multispectral Image (size: 396 $\times$ 184 $\times$ 4 res.: 5m $\times$ 5m) (c) Target (size: 396 $\times$ 184 $\times$ 224 res.: 5m $\times$ 5m)

Name	AVIRIS (HS)	SPOT-5 (MS)	Pleiades (MS)	WorldView-3 (MS)
Res. (m)	20	10	2	1.24
# bands	224	4	4	8

Table: Some existing remote sensors characteristics

Forward model for multi-band optical images

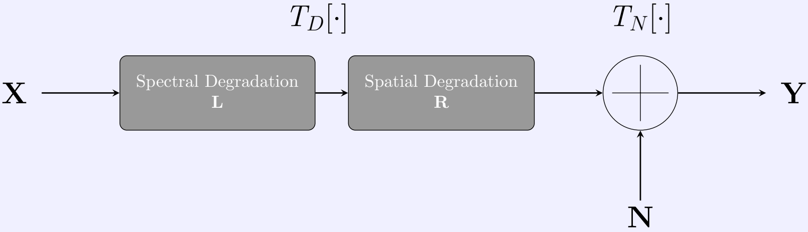

$$\mathbf{Y} = \mathbf{L}\mathbf{X}\mathbf{R} + \mathbf{N}$$

where

- **Y** observed multiband image of low spatial and/or spectral resolutions
  (row $\leftrightarrow$ band, column $\leftrightarrow$ pixel)
- **X** (unknown) latent image of high spatial and/or spectral resolutions
  (row $\leftrightarrow$ band, column $\leftrightarrow$ pixel)
- **L** spectral degradation matrix
- **R** spatial degradation matrix, e.g., decomposed as $\mathbf{R} = \mathbf{B}\mathbf{S}$ with
  - **B** spatial blur
  - **S** spatial subsampling

Complementary acquisitions: forward models

- $\mathbf{X} \in \mathbb{R}^{m_\lambda \times n}$: full resolution unknown image

$\mathbf{X}$

Complementary acquisitions: forward models

- **$\mathbf{X} \in \mathbb{R}^{m_\lambda \times n}$: full resolution unknown image**
- $\mathbf{B} \in \mathbb{R}^{n \times n}$: cyclic convolution operator acting on the bands

X

XB

Complementary acquisitions: forward models

- **$\mathbf{X} \in \mathbb{R}^{m_\lambda \times n}$: full resolution unknown image**

- $\mathbf{B} \in \mathbb{R}^{n \times n}$: cyclic convolution operator acting on the bands
- $\mathbf{S} \in \mathbb{R}^{n \times m}$: downsampling operator

X **XB** **XBS**

Complementary acquisitions: forward models

$$\mathbf{Y}_{\mathrm{H}} \approx \mathbf{XBS} \qquad ,$$

- $\mathbf{X} \in \mathbb{R}^{m_\lambda \times n}$: **full resolution unknown image**
- $\mathbf{Y}_{\mathrm{H}} \in \mathbb{R}^{m_\lambda \times m}$: observed HS image

- $\mathbf{B} \in \mathbb{R}^{n \times n}$: cyclic convolution operator acting on the bands
- $\mathbf{S} \in \mathbb{R}^{n \times m}$: downsampling operator

X **XB** **XBS**

Complementary acquisitions: forward models

$$\mathbf{Y}_{\mathrm{H}} \approx \mathbf{XBS} \qquad ,$$

- **$\mathbf{X} \in \mathbb{R}^{m_\lambda \times n}$: full resolution unknown image**
- $\mathbf{Y}_{\mathrm{H}} \in \mathbb{R}^{m_\lambda \times m}$: observed HS image

- $\mathbf{B} \in \mathbb{R}^{n \times n}$: cyclic convolution operator acting on the bands
- $\mathbf{S} \in \mathbb{R}^{n \times m}$: downsampling operator

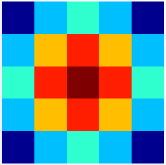

spatial blur **B**

Complementary acquisitions: forward models

$$\mathbf{Y}_{\mathrm{H}} \approx \mathbf{XBS} \qquad ,$$

- **$\mathbf{X} \in \mathbb{R}^{m_\lambda \times n}$: full resolution unknown image**
- $\mathbf{Y}_{\mathrm{H}} \in \mathbb{R}^{m_\lambda \times m}$: observed HS image

- $\mathbf{B} \in \mathbb{R}^{n \times n}$: cyclic convolution operator acting on the bands
- $\mathbf{S} \in \mathbb{R}^{n \times m}$: downsampling operator
- $\mathbf{R} \in \mathbb{R}^{n_\lambda \times m_\lambda}$: spectral response of the MS sensor

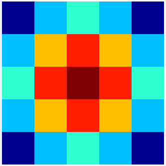

spatial blur **B**

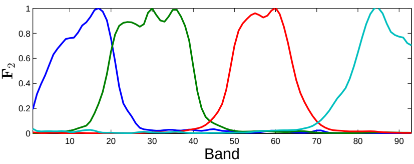

spectral response **R**

Complementary acquisitions: forward models

$$\mathbf{Y}_{\mathrm{H}} \approx \mathbf{XBS} \quad , \quad \mathbf{Y}_{\mathrm{M}} \approx \mathbf{RX}$$

- $\mathbf{X} \in \mathbb{R}^{m_\lambda \times n}$: **full resolution unknown image**
- $\mathbf{Y}_{\mathrm{H}} \in \mathbb{R}^{m_\lambda \times m}$: observed HS image
- $\mathbf{Y}_{\mathrm{M}} \in \mathbb{R}^{n_\lambda \times n}$: observed MS image
- $\mathbf{B} \in \mathbb{R}^{n \times n}$: cyclic convolution operator acting on the bands
- $\mathbf{S} \in \mathbb{R}^{n \times m}$: downsampling operator
- $\mathbf{R} \in \mathbb{R}^{n_\lambda \times m_\lambda}$: spectral response of the MS sensor

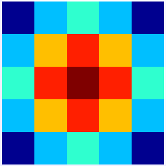

spatial blur **B**

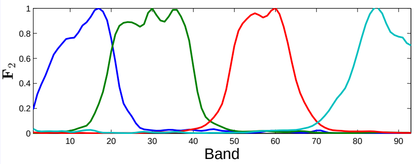

spectral response **R**

Complementary acquisitions: forward models

$$\mathbf{Y}_{\mathrm{H}} = \mathbf{XBS} + \mathbf{N}_{\mathrm{H}}, \quad \mathbf{Y}_{\mathrm{M}} = \mathbf{RX} + \mathbf{N}_{\mathrm{M}}$$

- **$\mathbf{X} \in \mathbb{R}^{m_\lambda \times n}$: full resolution unknown image**
- $\mathbf{Y}_{\mathrm{H}} \in \mathbb{R}^{m_\lambda \times m}$: observed HS image
- $\mathbf{Y}_{\mathrm{M}} \in \mathbb{R}^{n_\lambda \times n}$: observed MS image
- $\mathbf{B} \in \mathbb{R}^{n \times n}$: cyclic convolution operator acting on the bands
- $\mathbf{S} \in \mathbb{R}^{n \times m}$: downsampling operator
- $\mathbf{R} \in \mathbb{R}^{n_\lambda \times m_\lambda}$: spectral response of the MS sensor
- $\mathbf{N}_{\mathrm{H}} \in \mathbb{R}^{m_\lambda \times m}$ and $\mathbf{N}_{\mathrm{M}} \in \mathbb{R}^{n_\lambda \times n}$: HS and MS noises

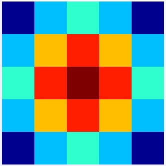

spatial blur **B**

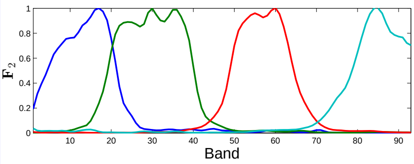

spectral response **R**

Noise statistics

Gaussian assumption

$$\mathbf{N}_{\mathrm{H}}|\mathbf{\Lambda}_{\mathrm{H}} \sim \mathcal{MN}_{m_\lambda,m}(\mathbf{0}_{m_\lambda,m}, \mathbf{\Lambda}_{\mathrm{H}}, \mathbf{I}_m)$$
$$\mathbf{N}_{\mathrm{M}}|\mathbf{\Lambda}_{\mathrm{M}} \sim \mathcal{MN}_{n_\lambda,n}(\mathbf{0}_{n_\lambda,n}, \mathbf{\Lambda}_{\mathrm{M}}, \mathbf{I}_n)$$

where

- $\mathbf{\Lambda}_{\mathrm{H}} = \mathrm{diag}\left\{s^2_{\mathrm{H},1}, \ldots, s^2_{\mathrm{H},m_\lambda}\right\}$ (hyperspectral noise variances)
- $\mathbf{\Lambda}_{\mathrm{M}} = \mathrm{diag}\left\{s^2_{\mathrm{M},1}, \ldots, s^2_{\mathrm{M},n_\lambda}\right\}$ (multispectral noise variances)

and the pdf of a matrix normal distribution is defined by

$$p(\mathbf{Z}|\bar{\mathbf{Z}}, \mathbf{\Sigma}_r, \mathbf{\Sigma}_c) \propto \exp\left(-\frac{1}{2}\,\mathrm{tr}\left[\mathbf{\Sigma}_c^{-1}(\mathbf{Z}-\bar{\mathbf{Z}})^T\mathbf{\Sigma}_r^{-1}(\mathbf{Z}-\bar{\mathbf{Z}})\right]\right)$$

$\rightarrow$ band-dependent noise

$\rightarrow$ pixel-independent noise

Likelihood of the observations

Given the forward model (characterized by both left- and right-operators)

$$\begin{aligned} \mathbf{Y}_{\mathrm{H}} &= \mathbf{XBS} + \mathbf{N}_{\mathrm{H}} \\ \mathbf{Y}_{\mathrm{M}} &= \mathbf{RX} + \mathbf{N}_{\mathrm{M}} \end{aligned}$$

the two likelihood functions express as

$$\begin{aligned} \mathbf{Y}_{\mathrm{H}}|\mathbf{X} &\sim \mathcal{MN}_{m_\lambda,m}(\mathbf{XBS}, \mathbf{\Lambda}_{\mathrm{H}}, \mathbf{I}_m) \\ \mathbf{Y}_{\mathrm{M}}|\mathbf{X} &\sim \mathcal{MN}_{n_\lambda,n}(\mathbf{RX}, \mathbf{\Lambda}_{\mathrm{M}}, \mathbf{I}_n) \end{aligned}$$

Joint likelihood
HS and MS images acquired by distinct sensors

- $\rightarrow$ independent HS and MS noises
- $\rightarrow$ independent observed images, cond. on $\mathbf{X}$

$$f(\mathbf{Y}_{\mathrm{H}}, \mathbf{Y}_{\mathrm{M}}|\mathbf{X}) = f(\mathbf{Y}_{\mathrm{H}}|\mathbf{X})\, f(\mathbf{Y}_{\mathrm{M}}|\mathbf{X})$$

Likelihood of the observations

Given the forward model (characterized by both left- and right-operators)

$$\mathbf{Y}_{\mathrm{H}} = \mathbf{XBS} + \mathbf{N}_{\mathrm{H}}$$
$$\mathbf{Y}_{\mathrm{M}} = \mathbf{RX} + \mathbf{N}_{\mathrm{M}}$$

the two likelihood functions express as

$$\mathbf{Y}_{\mathrm{H}}|\mathbf{X} \sim \mathcal{MN}_{m_\lambda,m}(\mathbf{XBS}, \mathbf{\Lambda}_{\mathrm{H}}, \mathbf{I}_m)$$
$$\mathbf{Y}_{\mathrm{M}}|\mathbf{X} \sim \mathcal{MN}_{n_\lambda,n}(\mathbf{RX}, \mathbf{\Lambda}_{\mathrm{M}}, \mathbf{I}_n)$$

Joint likelihood
HS and MS images acquired by distinct sensors

$\rightarrow$ independent HS and MS noises

$\rightarrow$ independent observed images, cond. on $\mathbf{X}$

$$f(\mathbf{Y}_{\mathrm{H}}, \mathbf{Y}_{\mathrm{M}}|\mathbf{X}) = f(\mathbf{Y}_{\mathrm{H}}|\mathbf{X})\, f(\mathbf{Y}_{\mathrm{M}}|\mathbf{X})$$

Multi-band image fusion as an estimation problem

Maximum likelihood estimation

Maximizing the two data-fitting terms writes

$$\hat{\mathbf{X}} \in \underset{\mathbf{X}}{\operatorname{argmin}} -\log f\left(\mathbf{Y}_{\mathrm{H}}|\mathbf{X}\right) - \log f\left(\mathbf{Y}_{\mathrm{M}}|\mathbf{X}\right)$$

formulated as a weighted least-square regression

$$\hat{\mathbf{X}} \in \underset{\mathbf{X}}{\operatorname{argmin}} \|\mathbf{Y}_{\mathrm{M}} - \mathbf{R}\mathbf{X}\|^2_{\mathbf{\Lambda}_{\mathrm{M}}^{-1}} + \|\mathbf{Y}_{\mathrm{H}} - \mathbf{X}\mathbf{B}\mathbf{S}\|^2_{\mathbf{\Lambda}_{\mathrm{H}}^{-1}}$$

Main issues

- (generally) large scale problem
- (generally) ill-posed (at least ill-conditioned) problem

Regularization required...

- (always) in the spectral domain
- (optional) in the spatial domain

Multi-band image fusion as an estimation problem

Maximum likelihood estimation

Maximizing the two data-fitting terms writes

$$\hat{\mathbf{X}} \in \operatorname*{argmin}_{\mathbf{X}} -\log f\left(\mathbf{Y}_{\mathrm{H}}|\mathbf{X}\right) - \log f\left(\mathbf{Y}_{\mathrm{M}}|\mathbf{X}\right)$$

formulated as a weighted least-square regression

$$\hat{\mathbf{X}} \in \operatorname*{argmin}_{\mathbf{X}} \|\mathbf{Y}_{\mathrm{M}} - \mathbf{R}\mathbf{X}\|^2_{\mathbf{\Lambda}_{\mathrm{M}}^{-1}} + \|\mathbf{Y}_{\mathrm{H}} - \mathbf{X}\mathbf{B}\mathbf{S}\|^2_{\mathbf{\Lambda}_{\mathrm{H}}^{-1}}$$

Main issues

- (generally) large scale problem
- (generally) ill-posed (at least ill-conditioned) problem

Regularization required...

- (always) in the spectral domain
- (optional) in the spatial domain

Spectral regularization
Low-rank representation

Hyperspectral pixels live in a (much) lower-dimensional subspace...

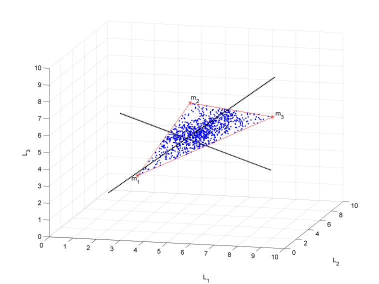

Unknown image **X** enforced to be decomposed as

$$\mathbf{X} = \mathbf{H}\mathbf{U}$$

i.e., its pixels live in a lower-dimensional subspace ($\mathbb{R}^{\widetilde{m}_\lambda}$ with $\widetilde{m}_\lambda \ll m_\lambda$) spanned by the columns of $\mathbf{H} \in \mathbb{R}^{m_\lambda \times \widetilde{m}_\lambda}$ (estimated or known a priori).

Spectral regularization
Low-rank representation

Hyperspectral pixels live in a (much) lower-dimensional subspace...

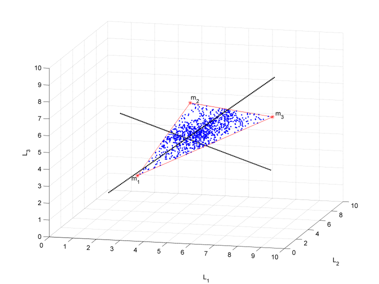

Unknown image **X** enforced to be decomposed as

$$\mathbf{X} = \mathbf{H}\mathbf{U}$$

i.e., its pixels live in a lower-dimensional subspace ($\mathbb{R}^{\widetilde{m}_\lambda}$ with $\widetilde{m}_\lambda \ll m_\lambda$) spanned by the columns of $\mathbf{H} \in \mathbb{R}^{m_\lambda \times \widetilde{m}_\lambda}$ (estimated or known a priori).

Optimization problem

Given the spectral regularization, the optimization problem writes

$$\hat{\mathbf{U}} \in \operatorname*{argmin}_{\mathbf{U}} \mathcal{J}(\mathbf{U})$$

with

$$\mathcal{J}(\mathbf{U}) = \left\| \mathbf{\Lambda}_{\mathrm{H}}^{-1} \left(\mathbf{Y}_{\mathrm{H}} - \mathbf{HUBS} \right) \right\|_{\mathrm{F}}^{2} + \left\| \mathbf{\Lambda}_{\mathrm{M}}^{-1} \left(\mathbf{Y}_{\mathrm{M}} - \mathbf{RHU} \right) \right\|_{\mathrm{F}}^{2}$$

$$\nabla \mathcal{J}(\mathbf{U}) = 0$$
$$\Leftrightarrow$$
finding $\mathbf{U}$ such that $\mathbf{C}_1 \mathbf{U} + \mathbf{U}\mathbf{C}_2 = \mathbf{C}_3$

with

$$\begin{aligned} \mathbf{C}_1 &= \left[\mathbf{H}^H \mathbf{\Lambda}_{\mathrm{H}}^{-1} \mathbf{H} \right]^{-1} \left[(\mathbf{RH})^H \mathbf{\Lambda}_{\mathrm{M}}^{-1} (\mathbf{RH}) \right] \\ \mathbf{C}_2 &= \left[\mathbf{BS} (\mathbf{BS})^H \right] \\ \mathbf{C}_3 &= \text{term depending on } \mathbf{Y}_{\mathrm{H}} \text{ and } \mathbf{Y}_{\mathrm{M}} \text{ (ind. on } \mathbf{U}\text{)} \end{aligned}$$

Solving a Sylvester matrix equation

$$\boxed{\mathbf{C}_1\mathbf{U} + \mathbf{U}\mathbf{C}_2 = \mathbf{C}_3}$$

Main issue
$\mathbf{C}_2 = \mathbf{BS}\,(\mathbf{BS})^H$ is not diagonalizable!

In the literature...

- *general resolution*: Bartels-Stewart algorithm (1972), with complexity of $\mathcal{O}(n^3)$
  $\rightarrow$ impossible in practice
- *in the context of fusion*: iterative algos, e.g., gradient descent, ADMM...
  $\rightarrow$ time consuming

Our contribution
We showed that an explicit solution can be written and easily computed! (see [WDT15a, WDT$^+$16])

Remark: result can be applied to (because generalizes) superresolution [ZWB$^+$16]...

Assumption 1

The blurring matrix $\mathbf{B}$ is a block circulant matrix with circulant blocks (BCCB).

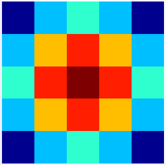

Assumption 2

The decimation matrix $\mathbf{S}$ corresponds to downsampling the original signal and its conjugate transpose $\mathbf{S}^H$ interpolates the decimated signal with zeros.

e.g.

$$\mathbf{S} = \begin{bmatrix} 1 & 0 & 0 & 0 & 1 & 0 & 0 & 0 & 1 & 0 & 0 & 0 & 1 & 0 & 0 & 0 \\ 0 & 1 & 0 & 0 & 0 & 1 & 0 & 0 & 0 & 1 & 0 & 0 & 0 & 1 & 0 & 0 \\ 0 & 0 & 1 & 0 & 0 & 0 & 1 & 0 & 0 & 0 & 1 & 0 & 0 & 0 & 1 & 0 \\ 0 & 0 & 0 & 1 & 0 & 0 & 0 & 1 & 0 & 0 & 0 & 1 & 0 & 0 & 0 & 1 \end{bmatrix}$$

Fast fUsion based on a Sylvester Equation (FUSE)

Input: $\mathbf{Y}_{\mathrm{M}}, \mathbf{Y}_{\mathrm{H}}, \boldsymbol{\Lambda}_{\mathrm{M}}, \boldsymbol{\Lambda}_{\mathrm{H}}, \mathbf{R}, \mathbf{B}, \mathbf{S}, \mathbf{H}$

$\mathbf{D} \leftarrow \mathbf{F}^{\mathbf{H}}\mathbf{B}\mathbf{F}$ and $\underline{\mathbf{D}} \leftarrow \mathbf{D}^*\mathbf{D}$ /* Circulant matrix: $\mathbf{B} = \mathbf{F}\mathbf{D}\mathbf{F}^H$ */

$\mathbf{C}_1 \leftarrow \left(\mathbf{H}^H\boldsymbol{\Lambda}_{\mathrm{H}}^{-1}\mathbf{H}\right)^{-1}\left((\mathbf{R}\mathbf{H})^H\boldsymbol{\Lambda}_{\mathrm{L}}^{-1}\mathbf{R}\mathbf{H}\right)$ /* Compute $\mathbf{C}_1$ */

$(\mathbf{Q}, \boldsymbol{\Lambda}_C) \leftarrow \mathrm{EigDec}(\mathbf{C}_1)$ /* Eigen-dec of $\mathbf{C}_1$: $\mathbf{C}_1 = \mathbf{Q}\boldsymbol{\Lambda}_C\mathbf{Q}^{-1}$ */

$\bar{\mathbf{C}}_3 \leftarrow \mathbf{Q}^{-1}\left(\mathbf{H}^H\boldsymbol{\Lambda}_{\mathrm{H}}^{-1}\mathbf{H}\right)^{-1}(\mathbf{H}^H\boldsymbol{\Lambda}_{\mathrm{H}}^{-1}\mathbf{Y}_{\mathrm{H}}(\mathbf{B}\mathbf{S})^H + (\mathbf{R}\mathbf{H})^H\boldsymbol{\Lambda}_{\mathrm{L}}^{-1}\mathbf{Y}_{\mathrm{M}})\mathbf{B}\mathbf{F}\mathbf{P}^{-1}$

for $l = 1$ **to** $\widetilde{m}_\lambda$ **do**

$$\underline{\mathbf{u}}_{l,1} = (\bar{\mathbf{C}}_3)_{l,1}\left(\frac{1}{d}\sum_{i=1}^{d}\underline{\mathbf{D}}_i + \lambda_C^l\mathbf{I}_n\right)^{-1}$$

for $j = 2$ **to** d **do**

$$\underline{\mathbf{u}}_{l,j} = \frac{1}{\lambda_C^l}\left((\bar{\mathbf{C}}_3)_{l,j} - \frac{1}{d}\underline{\mathbf{u}}_{l,1}\underline{\mathbf{D}}_j\right)$$

end

end

$\hat{\mathbf{U}} = \mathbf{Q}\underline{\mathbf{U}}\mathbf{P}\mathbf{D}^{-1}\mathbf{F}^H$

Output: $\hat{\mathbf{X}} = \mathbf{H}\hat{\mathbf{U}}$

From ML to MAP estimators

Incorporating (spatial) regularization

$$\hat{\mathbf{U}} \in \operatorname*{argmin}_{\mathbf{U}} \left\| \boldsymbol{\Lambda}_{\mathrm{H}}^{-1} \left(\mathbf{Y}_{\mathrm{H}} - \mathbf{HUBS}\right) \right\|_{\mathrm{F}}^{2} + \left\| \boldsymbol{\Lambda}_{\mathrm{M}}^{-1} \left(\mathbf{Y}_{\mathrm{M}} - \mathbf{RHU}\right) \right\|_{\mathrm{F}}^{2} + \mu \phi(\mathbf{U})$$

where

- $\phi(\mathbf{U}) = \left\| \boldsymbol{\Gamma} \left(\mathbf{U} - \bar{\mathbf{U}}\right) \right\|_{\mathrm{F}}^{2}$: (generalized) Thikonov regularizations
  - $\boldsymbol{\Gamma} = \mathbf{I}$ and $\bar{\mathbf{U}}$ =“crude estimate”: supervised naive Gaussian prior [WDT15b]
    $\rightarrow$ closed-form solution
  - joint estimation of $\underline{\boldsymbol{\Lambda}} = \{\boldsymbol{\Lambda}_{\mathrm{H}}, \boldsymbol{\Lambda}_{\mathrm{M}}\}$ and μ: unsupervised naive Gaussian prior [WDT15c]
    $\rightarrow$ closed-form solution embedded in BCD algorithm

From ML to MAP estimators

Incorporating (spatial) regularization

$$\hat{\mathbf{U}} \in \underset{\mathbf{U}}{\operatorname{argmin}} \left\| \mathbf{\Lambda}_{\mathrm{H}}^{-1} \left(\mathbf{Y}_{\mathrm{H}} - \mathbf{HUBS} \right) \right\|_{\mathrm{F}}^{2} + \left\| \mathbf{\Lambda}_{\mathrm{M}}^{-1} \left(\mathbf{Y}_{\mathrm{M}} - \mathbf{RHU} \right) \right\|_{\mathrm{F}}^{2} + \mu \phi(\mathbf{U})$$

where

- $\phi(\mathbf{U}) = \left\| \mathbf{\Gamma} \left(\mathbf{U} - \bar{\mathbf{U}} \right) \right\|_{\mathrm{F}}^{2}$: (generalized) Thikonov regularizations
  - $\mathbf{\Gamma} = \mathbf{I}$ and $\bar{\mathbf{U}}$ ="crude estimate": supervised naive Gaussian prior [WDT15b]
    $\rightarrow$ closed-form solution
  - joint estimation of $\underline{\mathbf{\Lambda}} = \{\mathbf{\Lambda}_{\mathrm{H}}, \mathbf{\Lambda}_{\mathrm{M}}\}$ and μ: unsupervised naive Gaussian prior [WDT15c]
    $\rightarrow$ closed-form solution embedded in BCD algorithm

Gaussian prior

Unsupervised naive Gaussian prior: closed-form solution embedded in BCD (FUSE-BCD)

Input: $\mathbf{Y}_{\mathrm{H}}, \mathbf{Y}_{\mathrm{M}}, \widetilde{m}_{\lambda}, \mathbf{B}, \mathbf{S}, \mathbf{R}, \mathbf{H}$
for $t = 1$ **to** T **do**
  // Optimize w.r.t. to $\mathbf{U}$
  $\mathbf{U}_t = \arg\min_{\mathbf{U}} L(\mathbf{U}, \underline{\mathbf{\Lambda}}_{t-1}, \mu_{t-1})$ /* Sylvester equation */
  // Optimize w.r.t. $\underline{\mathbf{\Lambda}}$
  $\underline{\mathbf{\Lambda}}_t = \arg\min_{\boldsymbol{s}^2} L(\mathbf{U}_t, \underline{\mathbf{\Lambda}}, \mu_{t-1})$
  // Optimize w.r.t. μ
  $\mu_t = \arg\min_{\mathbf{\Sigma}_{\boldsymbol{u}}} L(\mathbf{U}_t, \underline{\mathbf{\Lambda}}_t, \mu)$
end
$\hat{\mathbf{U}} \leftarrow \mathbf{U}_T$
Output: $\hat{\mathbf{X}} = \mathbf{H}\hat{\mathbf{U}}$

From ML to MAP estimators

Incorporating (spatial) regularization

$$\hat{\mathbf{U}} \in \underset{\mathbf{U}}{\operatorname{argmin}} \left\| \boldsymbol{\Lambda}_{\mathrm{H}}^{-1} \left(\mathbf{Y}_{\mathrm{H}} - \mathbf{HUBS} \right) \right\|_{\mathrm{F}}^{2} + \left\| \boldsymbol{\Lambda}_{\mathrm{M}}^{-1} \left(\mathbf{Y}_{\mathrm{M}} - \mathbf{RHU} \right) \right\|_{\mathrm{F}}^{2} + \mu \phi(\mathbf{U})$$

where

- $\phi(\mathbf{U}) = \left\| \boldsymbol{\Gamma} \left(\mathbf{U} - \bar{\mathbf{U}} \right) \right\|_{\mathrm{F}}^{2}$: (generalized) Thikonov regularizations
  - $\boldsymbol{\Gamma} = \mathbf{I}$ and $\bar{\mathbf{U}}$ =“crude estimate”: supervised naive Gaussian prior [WDT15b]
    $\rightarrow$ closed-form solution
  - joint estimation of $\underline{\boldsymbol{\Lambda}} = \{\boldsymbol{\Lambda}_{\mathrm{H}}, \boldsymbol{\Lambda}_{\mathrm{M}}\}$ and μ: unsupervised naive Gaussian prior [WDT15c]
    $\rightarrow$ closed-form solution embedded in BCD algorithm
- $\phi(\mathbf{U}) = \|\mathbf{U} - \mathbf{DA}\|_{\mathrm{F}}^{2}$: sparse representation based on dictionary learning [WBDT15]
  - $\mathbf{D}$: dictionary learnt beforehand
  - $\mathbf{A}$: code estimated (with sparse support learnt beforehand)

  $\rightarrow$ closed-form solution embedded in BCD algorithm

From ML to MAP estimators

Incorporating (spatial) regularization

$$\hat{\mathbf{U}} \in \operatorname*{argmin}_{\mathbf{U}} \left\| \boldsymbol{\Lambda}_{\mathrm{H}}^{-1} \left(\mathbf{Y}_{\mathrm{H}} - \mathbf{HUBS}\right) \right\|_{\mathrm{F}}^{2} + \left\| \boldsymbol{\Lambda}_{\mathrm{M}}^{-1} \left(\mathbf{Y}_{\mathrm{M}} - \mathbf{RHU}\right) \right\|_{\mathrm{F}}^{2} + \mu\phi(\mathbf{U})$$

where

- $\phi(\mathbf{U}) = \left\| \boldsymbol{\Gamma} \left(\mathbf{U} - \bar{\mathbf{U}} \right) \right\|_{\mathrm{F}}^{2}$: (generalized) Thikonov regularizations
  - $\boldsymbol{\Gamma} = \mathbf{I}$ and $\bar{\mathbf{U}}$ ="crude estimate": supervised naive Gaussian prior [WDT15b]
    $\rightarrow$ closed-form solution
  - joint estimation of $\underline{\boldsymbol{\Lambda}} = \{\boldsymbol{\Lambda}_{\mathrm{H}}, \boldsymbol{\Lambda}_{\mathrm{M}}\}$ and μ: unsupervised naive Gaussian prior [WDT15c]
    $\rightarrow$ closed-form solution embedded in BCD algorithm
- $\phi(\mathbf{U}) = \|\mathbf{U} - \mathbf{DA}\|_{\mathrm{F}}^{2}$: sparse representation based on dictionary learning [WBDT15]
  - **D**: dictionary learnt beforehand
  - **A**: code estimated (with sparse support learnt beforehand)

  $\rightarrow$ closed-form solution embedded in BCD algorithm

Sparse representation

Sparse prior: closed-form solution embedded in BCD (FUSE-BCD)

Input: $\mathbf{Y}_{\mathrm{H}}$, $\mathbf{Y}_{\mathrm{M}}$, $\widetilde{m}_{\lambda}$, $\mathbf{B}$, $\mathbf{S}$, $\mathbf{R}$, $\mathbf{H}$, $\mathrm{SNR}_{\mathrm{H}}$, $\mathrm{SNR}_{\mathrm{M}}$, $n_{\max}$

// Rough estimation of $\mathbf{U}$

Approximate $\bar{\mathbf{U}}$ using $\mathbf{Y}_{\mathrm{M}}$ and $\mathbf{Y}_{\mathrm{H}}$;

// Online dictionary learning

$\hat{\mathbf{D}} \leftarrow \mathrm{ODL}(\bar{\mathbf{U}})$;

// Sparse coding

$\hat{\mathbf{A}} \leftarrow \mathrm{OMP}(\hat{\mathbf{D}}, \bar{\mathbf{U}}, n_{\max})$;

// Computing support

$\hat{\mathbf{\Omega}} \leftarrow \hat{\mathbf{A}} \neq 0$;

// Start alternate optimization

for $t = 1$ **to** T **do**

  // Optimize w.r.t. to $\mathbf{U}$

  $\mathbf{U}_t = \arg\min_{\mathbf{U}} L(\mathbf{U}, \mathbf{A}_{t-1})$; /* Sylvester equation */

  // Optimize w.r.t. to $\mathbf{A}$

  $\mathbf{A}_t = \arg\min_{\mathbf{U}} L(\mathbf{U}_t, \mathbf{A})$; /* solved with LS */

end

Output: $\hat{\mathbf{X}} = \mathbf{H}\hat{\mathbf{U}}$

From ML to MAP estimators

Incorporating (spatial) regularization

$$\hat{\mathbf{U}} \in \operatorname*{argmin}_{\mathbf{U}} \left\| \boldsymbol{\Lambda}_{\mathrm{H}}^{-1} \left(\mathbf{Y}_{\mathrm{H}} - \mathbf{HUBS} \right) \right\|_{\mathrm{F}}^{2} + \left\| \boldsymbol{\Lambda}_{\mathrm{M}}^{-1} \left(\mathbf{Y}_{\mathrm{M}} - \mathbf{RHU} \right) \right\|_{\mathrm{F}}^{2} + \mu \phi(\mathbf{U})$$

where

- $\phi(\mathbf{U}) = \left\| \boldsymbol{\Gamma} \left(\mathbf{U} - \bar{\mathbf{U}} \right) \right\|_{\mathrm{F}}^{2}$: (generalized) Thikonov regularizations
  - $\boldsymbol{\Gamma} = \mathbf{I}$ and $\bar{\mathbf{U}}$ ="crude estimate": supervised naive Gaussian prior [WDT15b]
    $\rightarrow$ closed-form solution
  - joint estimation of $\underline{\boldsymbol{\Lambda}} = \{\boldsymbol{\Lambda}_{\mathrm{H}}, \boldsymbol{\Lambda}_{\mathrm{M}}\}$ and μ: unsupervised naive Gaussian prior [WDT15c]
    $\rightarrow$ closed-form solution embedded in BCD algorithm
- $\phi(\mathbf{U}) = \|\mathbf{U} - \mathbf{DA}\|_{\mathrm{F}}^{2}$: sparse representation based on dictionary learning [WBDT15]
  - $\mathbf{D}$: dictionary learnt beforehand
  - $\mathbf{A}$: code estimated (with sparse support learnt beforehand)

  $\rightarrow$ closed-form solution embedded in BCD algorithm
- $\phi(\mathbf{U}) = \sum_{j=1}^{\tilde{m}_\lambda} \mathrm{TV}\left[\mathbf{U}_{j,:}\right]$: band-wise total variation [SoBAC15]
  $\rightarrow$ closed-form solution embedded in ADMM algorithm

From ML to MAP estimators

Incorporating (spatial) regularization

$$\hat{\mathbf{U}} \in \underset{\mathbf{U}}{\operatorname{argmin}} \left\| \mathbf{\Lambda}_{\mathrm{H}}^{-1} \left(\mathbf{Y}_{\mathrm{H}} - \mathbf{HUBS} \right) \right\|_{\mathrm{F}}^2 + \left\| \mathbf{\Lambda}_{\mathrm{M}}^{-1} \left(\mathbf{Y}_{\mathrm{M}} - \mathbf{RHU} \right) \right\|_{\mathrm{F}}^2 + \mu \phi(\mathbf{U})$$

where

- $\phi(\mathbf{U}) = \left\| \mathbf{\Gamma} \left(\mathbf{U} - \bar{\mathbf{U}} \right) \right\|_{\mathrm{F}}^2$: (generalized) Thikonov regularizations
  - $\mathbf{\Gamma} = \mathbf{I}$ and $\bar{\mathbf{U}}$ =“crude estimate”: supervised naive Gaussian prior [WDT15b]
    $\rightarrow$ closed-form solution
  - joint estimation of $\underline{\mathbf{\Lambda}} = \{\mathbf{\Lambda}_{\mathrm{H}}, \mathbf{\Lambda}_{\mathrm{M}}\}$ and μ: unsupervised naive Gaussian prior [WDT15c]
    $\rightarrow$ closed-form solution embedded in BCD algorithm
- $\phi(\mathbf{U}) = \|\mathbf{U} - \mathbf{DA}\|_{\mathrm{F}}^2$: sparse representation based on dictionary learning [WBDT15]
  - **D**: dictionary learnt beforehand
  - **A**: code estimated (with sparse support learnt beforehand)

  $\rightarrow$ closed-form solution embedded in BCD algorithm
- $\phi(\mathbf{U}) = \sum_{j=1}^{\tilde{m}_\lambda} \mathrm{TV}\left[\mathbf{U}_{j,:}\right]$: band-wise total variation [SoBAC15]
  $\rightarrow$ closed-form solution embedded in ADMM algorithm

Non-Gaussian prior

Non-Gaussian prior, such as TV

$$\arg\min_{\mathbf{U}} \underbrace{\frac{1}{2}\|\mathbf{\Lambda}_{\mathrm{H}}^{-\frac{1}{2}}\left(\mathbf{Y}_{\mathrm{H}}-\mathbf{HUBS}\right)\|_{\mathrm{F}}^{2}}_{\text{HS data term}} + \underbrace{\frac{1}{2}\|\mathbf{\Lambda}_{\mathrm{M}}^{-\frac{1}{2}}\left(\mathbf{Y}_{\mathrm{M}}-\mathbf{RHU}\right)\|_{\mathrm{F}}^{2}}_{\text{MS data term}} + \underbrace{\lambda \mathrm{TV}\left(\mathbf{U}\right)}_{\text{regularizer}}.$$

can be equivalently solved as:

$$\arg\min_{\mathbf{U},\mathbf{V}} \frac{1}{2}\|\mathbf{\Lambda}_{\mathrm{H}}^{-\frac{1}{2}}\left(\mathbf{Y}_{\mathrm{H}}-\mathbf{HUBS}\right)\|_{F}^{2} + \frac{1}{2}\|\mathbf{\Lambda}_{\mathrm{M}}^{-\frac{1}{2}}\left(\mathbf{Y}_{\mathrm{M}}-\mathbf{RHU}\right)\|_{F}^{2} + \lambda \mathrm{TV}\left(\mathbf{V}\right) \text{ s.t. } \mathbf{U}=\mathbf{V}$$

- ADMM algorithm: alternate minimization (FUSE-ADMM)
  - closed-form solution of the Sylvester equation
  - proximal mapping

Illustrative results
PAN + HS fusion / Gaussian prior

(left to right) HS image, PAN image, ground truth, ADMM, proposed method.

Performance and computational times
HS + MS fusion / various regularizations

Table: RSNR (in dB), UIQI, SAM (in degree), ERGAS, DD (in 10^{-3}) and time (in second).

Regularization	Methods	RSNR	UIQI	SAM	ERGAS	DD	Time
supervised naive Gaussian	ADMM	29.321	0.9906	1.555	0.888	7.115	126.83
	FUSE	29.372	0.9908	1.551	0.879	7.092	0.38
unsupervised naive Gaussian	ADMM-BCD	29.084	0.9902	1.615	0.913	7.341	99.55
	FUSE-BCD	29.077	0.9902	1.623	0.913	7.368	1.09
sparse representation	ADMM-BCD	29.582	0.9911	1.423	0.872	6.678	162.88
	FUSE-BCD	29.688	0.9913	1.431	0.856	6.672	73.66
TV	ADMM	29.473	0.9912	1.503	0.861	6.922	134.21
	FUSE-ADMM	29.631	0.9915	1.477	0.845	6.788	90.99

- The computational time is decreased significantly!

Comparison with state-of-the-art methods
PAN + HS fusion

Table: Characteristics of the three datasets [LBDB+15]

dataset	dimensions	spatial res	N	instrument
Moffett	PAN 185 × 395 HS 37 × 79	20m 100m	224	AVIRIS
Camargue	PAN 500 × 500 HS 100 × 100	4m 20m	125	HyMap
Garons	PAN 400 × 400 HS 80 × 80	4m 20m	125	HyMap

Comparison with state-of-the-art methods

PAN + HS fusion

Table: Quality measures for the Moffett field dataset

method	CC	SAM	RMSE	ERGAS	Time(sec)
SFIM	0.92955	9.5271	365.2577	6.5429	1.26
MTF-GLP	0.93919	9.4599	352.1290	6.0491	1.86
MTF-GLP-HPM	0.93817	9.3567	354.8167	6.1992	1.71
GS	0.90521	14.1636	443.4351	7.5952	4.77
GSA	0.93857	11.2758	363.7090	6.2359	5.52
PCA	0.89580	14.6132	463.2204	7.9283	3.46
GFPCA	0.91614	11.3363	404.2979	7.0619	2.58
CNMF	0.95496	9.4177	314.4632	5.4200	10.98
Supervised Gaussian	0.97785	7.1308	220.0310	3.7807	1.31
Sparse represent.	0.98168	6.6392	200.3365	3.4281	133.61
HySure	0.97059	7.6351	254.2005	4.3582	140.05

Comparison with state-of-the-art methods

PAN + HS fusion

Table: Quality measures for the Camargue dataset

method	**CC**	**SAM**	**RMSE**	**ERGAS**	**Time**(sec)
SFIM	0.91886	4.2895	637.1451	3.4159	3.47
MTF-GLP	0.92397	4.3378	622.4711	3.2666	4.26
MTF-GLP-HPM	0.92599	4.2821	611.9161	3.2497	4.25
GS	0.91262	4.4982	665.0173	3.5490	8.29
GSA	0.92826	4.1950	587.1322	3.1940	8.73
PCA	0.90350	5.1637	710.3275	3.8680	8.92
GFPCA	0.89042	4.8472	745.6006	4.0001	8.51
CNMF	0.93000	4.4187	591.3190	3.1762	47.54
Supervised Gaussian	0.95195	3.6428	489.5634	2.6286	7.35
Sparse represent.	0.95882	3.3345	448.1721	2.4712	485.13
HySure	0.94650	3.8767	511.8525	2.8181	296.27

Comparison with state-of-the-art methods

PAN + HS fusion

Table: Quality measures for the Garons dataset

method	CC	SAM	RMSE	ERGAS	Time(sec)
SFIM	0.77052	6.7356	1036.4695	5.1702	2.74
MTF-GLP	0.80124	6.6155	956.3047	4.8245	4.00
MTF-GLP-HPM	0.79989	6.6905	962.1076	4.8280	2.98
GS	0.80347	6.6627	1037.6446	5.1373	5.56
GSA	0.80717	6.7719	928.6229	4.7076	5.99
PCA	0.81452	6.6343	1021.8547	5.0166	6.09
GFPCA	0.63390	7.4415	1312.0373	6.3416	4.36
CNMF	0.82993	6.9522	893.9194	4.4927	23.98
Supervised Gaussian	0.86857	5.8749	784.1298	3.9147	3.07
Sparse represent.	0.87834	5.6377	750.3510	3.7629	259.44
HySure	0.86080	6.0224	778.1051	4.0454	177.60

Outline

Introduction

Multi-band optical image fusion
- Problem statement
- Fast fusion solving a Sylvester equation
- Experiments

Multi-band optical image change detection
- Fusion approach
  - Problem statement
  - Resolution pipeline
  - Experiments
- Robust Fusion approach
  - Problem statement
  - Algorithm
  - Experimental results

Conclusions

Change Detection (CD)

Input

- Two or more multitemporal images.
- Same geographical spot (scene).

Output

- Change map.

Source: `RafaelRabellodeBarros`

CD in remote sensing context

Applications:

- Land-use and land-cover analysis.
- Urban monitoring.
- Environmental surveillance.
- Defense and security.

Taxonomy of methods:

- According to supervision.
  - Supervised.
  - Unsupervised.
- According to modality.
  - Same modality.
  - Multimodality.

Supervised vs. Unsupervised

Supervised

- Require ground information.
- More appropriate to multimodal images.
- Higher complexity of methods.
- Good overall performance.
- Depend on training set.
- Less appealing for real applications.

Unsupervised

- Does not require any ground information.
- Generally applied to same modalities.
- Lower complexity of methods.
- Lower overall performance.
- Generally require preprocessing steps.
- Automatic behaviour.

Favorable scenario

Landsat 8 04/15/2015 (PAN - 15m)

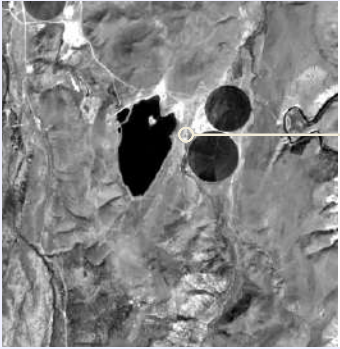

Landsat 8 09/22/2015 (PAN - 15m)

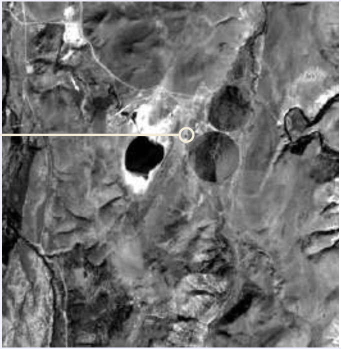

- Same modality.
- Identical resolutions.

Comparison of homologous pixels!

Same modality CD!

Favorable scenario

Landsat 8 04/15/2015 (PAN - 15m)

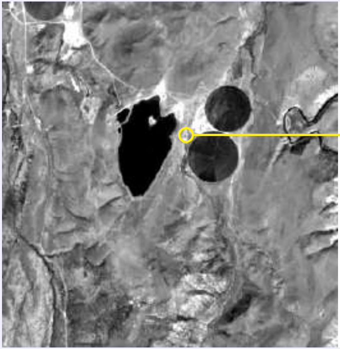

Landsat 8 09/22/2015 (PAN - 15m)

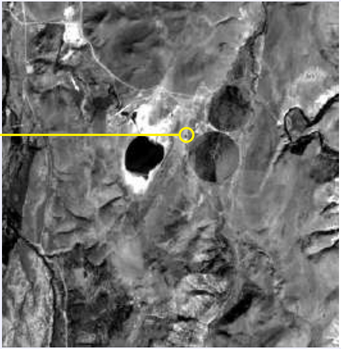

- Same modality.
- Identical resolutions.

Comparison of homologous pixels!

Same modality CD!

Unfavorable scenario

Emergence situation:
- Natural disaster.
- Punctual missions.
- Defense and security.

Need:
- Multimodal CD.

Landsat 8 04/15/2015 (MS - 30m)

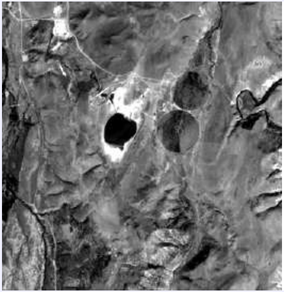

Landsat 8 09/22/2015 (PAN - 15m)

State-of-the-art

Principle:

- Identical resolutions obtained through independent and individual transformation over the considered images. [KCS+13]
- Multimodality CD achieved by supervised or semi-supervised methods [PCP+15].

Methods:

- Worst-case (WC): Degradation of both observed images.
- Degradation-Superresolution (DS): Spectral degradation followed by spatial Superresolution of LR-HS observed image.
- Superresolution-Degradation (SD): Spatial Superresolution followed by spectral degradation of LR-HS observed image.
- Coupled dictionary learning [GZSL16].

Problems:

- No joint processing.
- Loss of information (DS and SD).
- Loss of resolution (WC).

Adopted strategy: leveraging on fusion

General principle:

- Consider two images of same region acquired at same time (no change).
- Fused image evidences information contained in the pair of input images.
- Able to deal with different resolutions (e.g. pansharpening).

Today:

- Fusion-based approach [FDWC18]
- Robust-fusion based approach [FDWC17]

Remarks:

- Easier to manipulate optical images due to the noise statistics.
- 85% of the total earth observation satellites are optical [oCS17].

Forward model for multi-band optical images

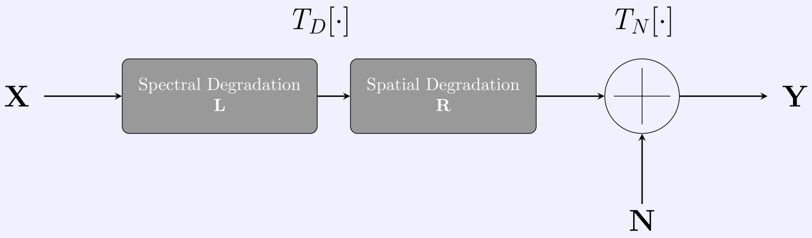

$$\mathbf{Y} = \mathbf{LXR} + \mathbf{N}$$

where

- **Y** observed multiband image of low spatial and/or spectral resolutions
  (row $\leftrightarrow$ band, column $\leftrightarrow$ pixel)
- **X** (unknown) latent image of high spatial and/or spectral resolutions
  (row $\leftrightarrow$ band, column $\leftrightarrow$ pixel)
- **L** spectral degradation matrix
- **R** spatial degradation matrix, e.g., decomposed as $\mathbf{R} = \mathbf{BS}$ with
  - **B** spatial blur
  - **S** spatial subsampling

Applicative scenarios

	Forward model ♯1		Forward model ♯2		Comments
	Spectral degradation	Spatial degradation	Spectral degradation	Spatial degradation	
$\mathcal{S}_1$	–	–	–	–	Conventional CD framework – $\mathbf{Y}_1$ and $\mathbf{Y}_2$ of same spatial and spectral resolutions
$\mathcal{S}_2$	$\mathbf{L}_1$	–	–	–	$\mathbf{Y}_1$ of lower spectral resolution $\mathbf{Y}_1$ and $\mathbf{Y}_2$ of same spatial resolutions
$\mathcal{S}_3$	–	$\mathbf{R}_1$	–	–	$\mathbf{Y}_1$ of lower spatial resolution $\mathbf{Y}_1$ and $\mathbf{Y}_2$ of same spectral resolutions
$\mathcal{S}_4$	–	$\mathbf{R}_1$	$\mathbf{L}_2$	–	$\mathbf{Y}_1$ and $\mathbf{Y}_2$ of complementary resolutions
$\mathcal{S}_5$	$\mathbf{L}_1$	$\mathbf{R}_1$	–	–	$\mathbf{Y}_1$ of low spatial and spectral resolutions
$\mathcal{S}_6$	–	$\mathbf{R}_1$	–	$\mathbf{R}_2$	Generalization of $\mathcal{S}_3$ with non-integer relative spatial downsampling factor
$\mathcal{S}_7$	$\mathbf{L}_1$	$\mathbf{R}_1$	–	$\mathbf{R}_2$	Generalization of $\mathcal{S}_4$ with non-integer relative spatial downsampling factor
$\mathcal{S}_8$	$\mathbf{L}_1$	–	$\mathbf{L}_2$	–	Generalization of $\mathcal{S}_2$ with some non-overlapping spectral bands
$\mathcal{S}_9$	$\mathbf{L}_1$	$\mathbf{R}_1$	$\mathbf{L}_2$	–	Generalization of $\mathcal{S}_4$ with some non-overlapping spectral bands
$\mathcal{S}_{10}$	$\mathbf{L}_1$	$\mathbf{R}_1$	$\mathbf{L}_2$	$\mathbf{R}_2$	Generalization of $\mathcal{S}_4$ with some non-overlapping spectral bands and non-integer relative spatial downsampling factor

Table: Overview of the spectral and spatial degradations w.r.t. experimental scenarios. The symbol – stands for “no degradation” [FDC20].

Applicative scenarios

	Forward model $\sharp 1$		Forward model $\sharp 2$		Comments
	Spectral degradation	Spatial degradation	Spectral degradation	Spatial degradation	
$\mathcal{S}_1$	–	–	–	–	Conventional CD framework – $\mathbf{Y}_1$ and $\mathbf{Y}_2$ of same spatial and spectral resolutions
$\mathcal{S}_2$	$\mathbf{L}_1$	–	–	–	$\mathbf{Y}_1$ of lower spectral resolution $\mathbf{Y}_1$ and $\mathbf{Y}_2$ of same spatial resolutions
$\mathcal{S}_3$	–	$\mathbf{R}_1$	–	–	$\mathbf{Y}_1$ of lower spatial resolution $\mathbf{Y}_1$ and $\mathbf{Y}_2$ of same spectral resolutions
$\mathcal{S}_4$	–	$\mathbf{R}_1$	$\mathbf{L}_2$	–	$\mathbf{Y}_1$ and $\mathbf{Y}_2$ of complementary resolutions
$\mathcal{S}_5$	$\mathbf{L}_1$	$\mathbf{R}_1$	–	–	$\mathbf{Y}_1$ of low spatial and spectral resolutions
$\mathcal{S}_6$	–	$\mathbf{R}_1$	–	$\mathbf{R}_2$	Generalization of $\mathcal{S}_3$ with non-integer relative spatial downsampling factor
$\mathcal{S}_7$	$\mathbf{L}_1$	$\mathbf{R}_1$	–	$\mathbf{R}_2$	Generalization of $\mathcal{S}_4$ with non-integer relative spatial downsampling factor
$\mathcal{S}_8$	$\mathbf{L}_1$	–	$\mathbf{L}_2$	–	Generalization of $\mathcal{S}_2$ with some non-overlapping spectral bands
$\mathcal{S}_9$	$\mathbf{L}_1$	$\mathbf{R}_1$	$\mathbf{L}_2$	–	Generalization of $\mathcal{S}_4$ with some non-overlapping spectral bands
$\mathcal{S}_{10}$	$\mathbf{L}_1$	$\mathbf{R}_1$	$\mathbf{L}_2$	$\mathbf{R}_2$	Generalization of $\mathcal{S}_4$ with some non-overlapping spectral bands and non-integer relative spatial downsampling factor

Table: Overview of the spectral and spatial degradations w.r.t. experimental scenarios. The symbol – stands for “no degradation” [FDC20].

Scenario $\mathcal{S}_4$

Landsat 8 04/15/2015 (MS - 30m)

$\mathbf{Y}_{\text{LR}} = \mathbf{X}\mathbf{R} + \mathbf{N}_{\text{LR}}$

Landsat 8 09/22/2015 (PAN - 15m)

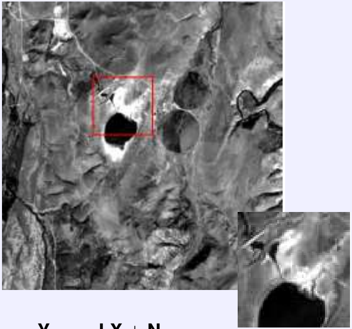

$\mathbf{Y}_{\text{HR}} = \mathbf{L}\mathbf{X} + \mathbf{N}_{\text{HR}}$

- Time ordering independent: $t_1 \neq t_2$.

Problem statement

Joint observation model

$$\mathbf{Y}_{\mathrm{LR}} = \mathbf{X}\mathbf{R} + \mathbf{N}_{\mathrm{LR}}$$
$$\mathbf{Y}_{\mathrm{HR}} = \mathbf{L}\mathbf{X} + \mathbf{N}_{\mathrm{HR}}$$

Fusion process

$$\hat{\mathbf{X}} \leftarrow \mathrm{FUSION}\left(\mathbf{Y}_{\mathrm{LR}}, \mathbf{Y}_{\mathrm{HR}}\right)$$

"Predicted" pseudo-observed images

$$\hat{\mathbf{Y}}_{\mathrm{LR}} \triangleq \hat{\mathbf{X}}\mathbf{R}$$
$$\hat{\mathbf{Y}}_{\mathrm{HR}} \triangleq \mathbf{L}\hat{\mathbf{X}}$$

Fusion properties [LdBD+15, WRM97]

- *Synthesis*: fused image ≈ image obtained by the sensor of the target resolution.
- *Consistency*: reversibility of the fusion process.

Consistency-based CD hypothesis testing

$$\mathcal{H}_0 : \begin{cases} \mathbf{Y}_{\mathrm{LR}} = \hat{\mathbf{Y}}_{\mathrm{LR}} \\ \mathbf{Y}_{\mathrm{HR}} = \hat{\mathbf{Y}}_{\mathrm{HR}} \end{cases} \quad \text{(no change)}$$

$$\mathcal{H}_1 : \begin{cases} \mathbf{Y}_{\mathrm{LR}} \neq \hat{\mathbf{Y}}_{\mathrm{LR}} \\ \mathbf{Y}_{\mathrm{HR}} \neq \hat{\mathbf{Y}}_{\mathrm{HR}} \end{cases} \quad \text{(change)}$$

Problem statement

Joint observation model

$$\begin{aligned}\mathbf{Y}_{\mathrm{LR}} &= \mathbf{X}\mathbf{R} + \mathbf{N}_{\mathrm{LR}}\\ \mathbf{Y}_{\mathrm{HR}} &= \mathbf{L}\mathbf{X} + \mathbf{N}_{\mathrm{HR}}\end{aligned}$$

Fusion process

$$\hat{\mathbf{X}} \leftarrow \mathrm{FUSION}\left(\mathbf{Y}_{\mathrm{LR}}, \mathbf{Y}_{\mathrm{HR}}\right)$$

"Predicted" pseudo-observed images

$$\begin{aligned}\hat{\mathbf{Y}}_{\mathrm{LR}} &\triangleq \hat{\mathbf{X}}\mathbf{R}\\ \hat{\mathbf{Y}}_{\mathrm{HR}} &\triangleq \mathbf{L}\hat{\mathbf{X}}\end{aligned}$$

Fusion properties [LdBD+15, WRM97]

- *Synthesis*: fused image $\approx$ image obtained by the sensor of the target resolution.
- *Consistency*: reversibility of the fusion process.

Consistency-based CD hypothesis testing

$$\mathcal{H}_0 : \begin{cases} \mathbf{Y}_{\mathrm{LR}} = \hat{\mathbf{Y}}_{\mathrm{LR}} \\ \mathbf{Y}_{\mathrm{HR}} = \hat{\mathbf{Y}}_{\mathrm{HR}} \end{cases} \quad \text{(no change)}$$

$$\mathcal{H}_1 : \begin{cases} \mathbf{Y}_{\mathrm{LR}} \neq \hat{\mathbf{Y}}_{\mathrm{LR}} \\ \mathbf{Y}_{\mathrm{HR}} \neq \hat{\mathbf{Y}}_{\mathrm{HR}} \end{cases} \quad \text{(change)}$$

Problem statement

Joint observation model

$$\mathbf{Y}_{\mathrm{LR}} = \mathbf{X}\mathbf{R} + \mathbf{N}_{\mathrm{LR}}$$
$$\mathbf{Y}_{\mathrm{HR}} = \mathbf{L}\mathbf{X} + \mathbf{N}_{\mathrm{HR}}$$

Fusion process

$$\hat{\mathbf{X}} \leftarrow \mathrm{FUSION}\left(\mathbf{Y}_{\mathrm{LR}}, \mathbf{Y}_{\mathrm{HR}}\right)$$

"Predicted" pseudo-observed images

$$\hat{\mathbf{Y}}_{\mathrm{LR}} \triangleq \hat{\mathbf{X}}\mathbf{R}$$
$$\hat{\mathbf{Y}}_{\mathrm{HR}} \triangleq \mathbf{L}\hat{\mathbf{X}}$$

Fusion properties [LdBD+15, WRM97]

- *Synthesis*: fused image ≈ image obtained by the sensor of the target resolution.
- *Consistency*: reversibility of the fusion process.

Consistency-based CD hypothesis testing

$$\mathcal{H}_0 : \begin{cases} \mathbf{Y}_{\mathrm{LR}} = \hat{\mathbf{Y}}_{\mathrm{LR}} \\ \mathbf{Y}_{\mathrm{HR}} = \hat{\mathbf{Y}}_{\mathrm{HR}} \end{cases} \quad \text{(no change)}$$

$$\mathcal{H}_1 : \begin{cases} \mathbf{Y}_{\mathrm{LR}} \neq \hat{\mathbf{Y}}_{\mathrm{LR}} \\ \mathbf{Y}_{\mathrm{HR}} \neq \hat{\mathbf{Y}}_{\mathrm{HR}} \end{cases} \quad \text{(change)}$$

Problem statement

Joint observation model

$$\begin{aligned}\mathbf{Y}_{\mathrm{LR}} &= \quad \mathbf{XR} + \mathbf{N}_{\mathrm{LR}} \\ \mathbf{Y}_{\mathrm{HR}} &= \mathbf{LX} \quad + \mathbf{N}_{\mathrm{HR}}\end{aligned}$$

Fusion process

$$\hat{\mathbf{X}} \leftarrow \mathrm{FUSION}\left(\mathbf{Y}_{\mathrm{LR}}, \mathbf{Y}_{\mathrm{HR}}\right)$$

"Predicted" pseudo-observed images

$$\begin{aligned}\hat{\mathbf{Y}}_{\mathrm{LR}} &\triangleq \hat{\mathbf{X}}\mathbf{R} \\ \hat{\mathbf{Y}}_{\mathrm{HR}} &\triangleq \mathbf{L}\hat{\mathbf{X}}\end{aligned}$$

Fusion properties [LdBD+15, WRM97]

- *Synthesis*: fused image $\approx$ image obtained by the sensor of the target resolution.
- *Consistency*: reversibility of the fusion process.

Consistency-based CD hypothesis testing

$$\mathcal{H}_0 : \begin{cases} \mathbf{Y}_{\mathrm{LR}} = \hat{\mathbf{Y}}_{\mathrm{LR}} \\ \mathbf{Y}_{\mathrm{HR}} = \hat{\mathbf{Y}}_{\mathrm{HR}} \end{cases} \quad \text{(no change)}$$

$$\mathcal{H}_1 : \begin{cases} \mathbf{Y}_{\mathrm{LR}} \neq \hat{\mathbf{Y}}_{\mathrm{LR}} \\ \mathbf{Y}_{\mathrm{HR}} \neq \hat{\mathbf{Y}}_{\mathrm{HR}} \end{cases} \quad \text{(change)}$$

3-steps procedure [FDWC18]

1. *fusion*: estimating $\hat{\mathbf{X}}$ from $\mathbf{Y}_{\mathrm{LR}}$ and $\mathbf{Y}_{\mathrm{HR}}$
   - Tailored by the end user [FYDC18]
     e.g., Fast fusion based on solving a SE

2. *prediction*: reconstructing $\hat{\mathbf{Y}}_{\mathrm{LR}}$ and $\hat{\mathbf{Y}}_{\mathrm{HR}}$ from $\hat{\mathbf{X}}$

$$\begin{aligned}\hat{\mathbf{Y}}_{\mathrm{LR}} &= \hat{\mathbf{X}}\mathbf{R}\\ \hat{\mathbf{Y}}_{\mathrm{HR}} &= \mathbf{L}\hat{\mathbf{X}}.\end{aligned}$$

3. *decision*: deriving change maps $\hat{\mathbf{D}}_{\mathrm{LR}}$ and $\hat{\mathbf{D}}_{\mathrm{HR}}$ from, resp.,

$$\Upsilon_{\mathrm{LR}} = \left\{\mathbf{Y}_{\mathrm{LR}}, \hat{\mathbf{Y}}_{\mathrm{LR}}\right\},$$

$$\Upsilon_{\mathrm{HR}} = \left\{\mathbf{Y}_{\mathrm{HR}}, \hat{\mathbf{Y}}_{\mathrm{HR}}\right\}.$$

   - Tailored by the end user.
     e.g., Change Vector Analysis (CVA) [BB07]

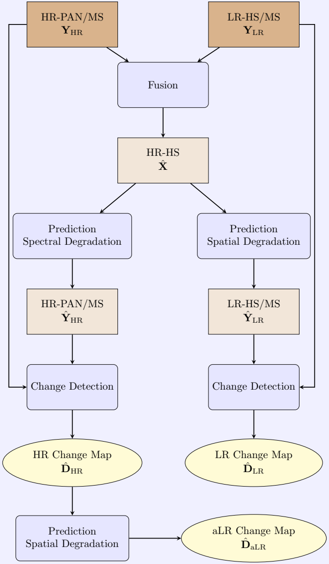

Experiments on synthetic images

Detection performance

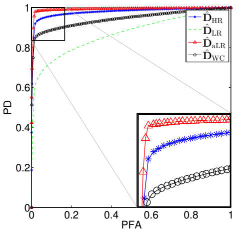

(a) Situation 1: HR-MS/LR-HS

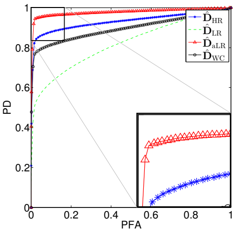

(b) Situation 2: HR-PAN/LR-HS

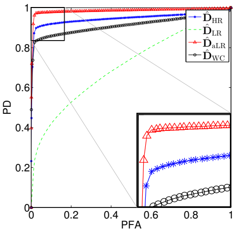

(c) Situation 3: HR-PAN/LR-MS

Table: Situations 1, 2 & 3: quantitative detection performance (AUC and distance).

		$\hat{\mathbf{D}}_{\mathrm{HR}}$	$\hat{\mathbf{D}}_{\mathrm{LR}}$	$\hat{\mathbf{D}}_{\mathrm{aLR}}$	$\hat{\mathbf{D}}_{\mathrm{WC}}$
Situation 1	AUC	0.981039	0.867478	**0.992242**	0.941408
	Dist.	0.951995	0.789379	**0.979298**	0.887789
Situation 2	AUC	0.931047	0.819679	**0.977362**	0.89517
	Dist.	0.883488	0.737274	**0.952995**	0.833783
Situation 3	AUC	0.94522	0.711167	**0.984833**	0.911311
	Dist.	0.915992	0.647865	**0.972997**	0.864686

Experiments on real images
Data description

Observed image at t_1 (04/15/2015):

- Local: Lake-Tahoe (CA) USA.
- Sensor: Landsat 8.
- Image size: 175 $\times$ 180 pixels.
- Spatial resolution: 30m per pixel.
- Spectral resolution: 3 spectral bands (MS) in RBG visible spectrum.

Observed image at t_2 (09/22/2015):

- Local: Lake-Tahoe (CA) USA.
- Sensor: Landsat 8.
- Image size: 350 $\times$ 360 pixels.
- Spatial resolution: 15m per pixel.
- Spectral resolution: PAN in RBG visible spectrum.

Preprocessing:

- Manual alignment.

Compared Methods:

- Fusion approach ($\hat{\mathbf{D}}_{\mathrm{HR}}, \hat{\mathbf{D}}_{\mathrm{aLR}}$) .
- Worst-case approach ($\hat{\mathbf{D}}_{\mathrm{WC}}$).

Experiments on real images

Visual results

(a) $\mathbf{Y}_{\mathrm{LR}}$ (b) $\mathbf{Y}_{\mathrm{HR}}$ (c) $\hat{\mathbf{D}}_{\mathrm{HR}}$ (d) $\hat{\mathbf{D}}_{\mathrm{aLR}}$ (e) $\hat{\mathbf{D}}_{\mathrm{WC}}$

(f) zoomed $\mathbf{Y}_{\mathrm{LR}}$ (g) zoomed $\mathbf{Y}_{\mathrm{HR}}$ (h) zoomed $\hat{\mathbf{D}}_{\mathrm{HR}}$ (i) zoomed $\hat{\mathbf{D}}_{\mathrm{aLR}}$ (j) zoomed $\hat{\mathbf{D}}_{\mathrm{WC}}$

Real scenario (LR-MS and HR-PAN): (a) LR-MS observed image $\mathbf{Y}_{\mathrm{LR}}$, (b) HR-PAN observed image $\mathbf{Y}_{\mathrm{HR}}$, (c) change mask $\hat{\mathbf{D}}_{\mathrm{HR}}$, (d) change mask $\hat{\mathbf{D}}_{\mathrm{aLR}}$, (e) change mask $\hat{\mathbf{D}}_{\mathrm{WC}}$ estimated by the worst-case approach. From (f) to (j): zoomed versions of the regions delineated in red in (a)–(e).

Problem statement

Joint observation model: from fusion...

$$
\begin{aligned}
\mathbf{Y}_{\mathrm{LR}} &= \mathbf{X}\,\mathbf{R} + \mathbf{N}_{\mathrm{LR}} \\
\mathbf{Y}_{\mathrm{HR}} &= \mathbf{L}\mathbf{X} + \mathbf{N}_{\mathrm{HR}}
\end{aligned}
$$

with

- $\mathbf{X}_1$: latent image at t_1
- $\mathbf{X}_2$: latent image at t_2

or, equivalently, $\mathbf{X}_2 = \mathbf{X}_1 + \Delta\mathbf{X}$ with

- $\Delta\mathbf{X}$: change image

$$\Delta\mathbf{X} = [\Delta\mathbf{x}_1, \ldots, \Delta\mathbf{x}_n] \text{ and } \Delta\mathbf{x}_i = \left[\Delta x_{1,i}, \ldots, \Delta x_{m_\lambda,i}\right]^T$$

CD hypothesis testing

Decision rule for the ith pixel ($i = 1, \ldots, n$)

$$
\begin{aligned}
\mathcal{H}_0 &: \|\Delta\mathbf{x}_i\|_2 < \tau \quad \text{(no change)} \\
\mathcal{H}_1 &: \|\Delta\mathbf{x}_i\|_2 \geq \tau \quad \text{(change)}
\end{aligned}
$$

Problem statement

*Joint observation model: from fusion... to **robust** fusion*

$$\begin{aligned} \mathbf{Y}_{\mathrm{LR}} &= \mathbf{X}_1\mathbf{R} + \mathbf{N}_{\mathrm{LR}} \\ \mathbf{Y}_{\mathrm{HR}} &= \mathbf{L}\mathbf{X}_2 + \mathbf{N}_{\mathrm{HR}} \end{aligned}$$

with

- $\mathbf{X}_1$: latent image at t_1
- $\mathbf{X}_2$: latent image at t_2

or, equivalently, $\mathbf{X}_2 = \mathbf{X}_1 + \Delta\mathbf{X}$ with

- $\Delta\mathbf{X}$: change image

$$\Delta\mathbf{X} = [\Delta\mathbf{x}_1, \ldots, \Delta\mathbf{x}_n] \text{ and } \Delta\mathbf{x}_i = \left[\Delta x_{1,i}, \ldots, \Delta x_{m_\lambda,i}\right]^T$$

CD hypothesis testing

Decision rule for the ith pixel ($i = 1, \ldots, n$)

$$\begin{aligned} \mathcal{H}_0 &: \|\Delta\mathbf{x}_i\|_2 < \tau \quad \text{(no change)} \\ \mathcal{H}_1 &: \|\Delta\mathbf{x}_i\|_2 \geq \tau \quad \text{(change)} \end{aligned}$$

Problem statement

*Joint observation model: from fusion... to **robust** fusion*

$$\begin{aligned}\mathbf{Y}_{\mathrm{LR}} &= \mathbf{X}_1\mathbf{R} + \mathbf{N}_{\mathrm{LR}}\\ \mathbf{Y}_{\mathrm{HR}} &= \mathbf{L}\mathbf{X}_2 + \mathbf{N}_{\mathrm{HR}}\end{aligned}$$

with

- $\mathbf{X}_1$: latent image at t_1
- $\mathbf{X}_2$: latent image at t_2

or, equivalently, $\mathbf{X}_2 = \mathbf{X}_1 + \Delta\mathbf{X}$ with

- $\Delta\mathbf{X}$: change image

$$\Delta\mathbf{X} = [\Delta\mathbf{x}_1, \ldots, \Delta\mathbf{x}_n] \text{ and } \Delta\mathbf{x}_i = \left[\Delta x_{1,i}, \ldots, \Delta x_{m_\lambda,i}\right]^T$$

CD hypothesis testing

Decision rule for the ith pixel ($i = 1, \ldots, n$)

$$\mathcal{H}_0 : \|\Delta\mathbf{x}_i\|_2 < \tau \quad \text{(no change)}$$

$$\mathcal{H}_1 : \|\Delta\mathbf{x}_i\|_2 \geq \tau \quad \text{(change)}$$

Problem statement

*Joint observation model: from fusion... to **robust** fusion*

$$\begin{aligned}\mathbf{Y}_{\mathrm{LR}} &= \mathbf{X}_1\mathbf{R} + \mathbf{N}_{\mathrm{LR}}\\ \mathbf{Y}_{\mathrm{HR}} &= \mathbf{L}\mathbf{X}_2 + \mathbf{N}_{\mathrm{HR}}\end{aligned}$$

with

- $\mathbf{X}_1$: latent image at t_1
- $\mathbf{X}_2$: latent image at t_2

or, equivalently, $\mathbf{X}_2 = \mathbf{X}_1 + \Delta\mathbf{X}$ with

- $\Delta\mathbf{X}$: change image

$$\Delta\mathbf{X} = [\Delta\mathbf{x}_1, \ldots, \Delta\mathbf{x}_n] \text{ and } \Delta\mathbf{x}_i = \left[\Delta x_{1,i}, \ldots, \Delta x_{m_\lambda,i}\right]^T$$

CD hypothesis testing

Decision rule for the ith pixel ($i = 1, \ldots, n$)

$$\begin{aligned}\mathcal{H}_0 &: \|\Delta\mathbf{x}_i\|_2 < \tau \quad \text{(no change)}\\ \mathcal{H}_1 &: \|\Delta\mathbf{x}_i\|_2 \geq \tau \quad \text{(change)}\end{aligned}$$

Optimization problem

Likelihood of the observations

$$\mathbf{Y}_{\mathrm{LR}}|\mathbf{X}_1 \sim \mathcal{MN}_{n_\lambda, m_1}(\mathbf{X}_1\mathbf{R}, \mathbf{\Lambda}_{\mathrm{LR}}, \mathbf{I}_{m_1})$$
$$\mathbf{Y}_{\mathrm{HR}}|\mathbf{X}_2 \sim \mathcal{MN}_{m_{\lambda_2}, n}(\mathbf{L}\mathbf{X}_2, \mathbf{\Lambda}_{\mathrm{HR}}, \mathbf{I}_n)$$

Maximum a posteriori (MAP) estimator

$$\begin{aligned}\left\{\hat{\mathbf{X}}_{1,\mathrm{MAP}}, \Delta\hat{\mathbf{X}}_{\mathrm{MAP}}\right\} \in \arg\min_{\mathbf{X}_1, \Delta\mathbf{X}} & \left\|\mathbf{\Lambda}_{\mathrm{LR}}^{-\frac{1}{2}}\left(\mathbf{Y}_{\mathrm{LR}} - \mathbf{X}_1\mathbf{R}\right)\right\|_F^2 \\ & + \left\|\mathbf{\Lambda}_{\mathrm{HR}}^{-\frac{1}{2}}\left(\mathbf{Y}_{\mathrm{HR}} - \mathbf{L}\left(\mathbf{X}_1 + \Delta\mathbf{X}\right)\right)\right\|_F^2 \\ & + \mu\phi_1\left(\mathbf{X}_1\right) + \gamma\phi_2\left(\Delta\mathbf{X}\right)\end{aligned}$$

Key ingredient: ϕ_2

Spatial sparsity of the changes through a group-lasso regularization

$$\begin{aligned}\phi_2\left(\Delta\mathbf{X}\right) &= \left\|\Delta\mathbf{X}\right\|_{2,1} \\ &= \sum_{i=1}^{n}\left\|\Delta\mathbf{x}_i\right\|_2 = \left\|\mathbf{e}\right\|_1\end{aligned}$$

promoting a sparse change image energy vector $\mathbf{e} = \left[\left\|\Delta\mathbf{x}_1\right\|_2, \ldots, \left\|\Delta\mathbf{x}_n\right\|_2\right]$.

Optimization problem

Likelihood of the observations

$$\mathbf{Y}_{\mathrm{LR}}|\mathbf{X}_1 \sim \mathcal{MN}_{n_\lambda, m_1}(\mathbf{X}_1\mathbf{R}, \mathbf{\Lambda}_{\mathrm{LR}}, \mathbf{I}_{m_1})$$
$$\mathbf{Y}_{\mathrm{HR}}|\mathbf{X}_2 \sim \mathcal{MN}_{m_{\lambda_2}, n}(\mathbf{L}\mathbf{X}_2, \mathbf{\Lambda}_{\mathrm{HR}}, \mathbf{I}_n)$$

Maximum a posteriori (MAP) estimator

$$\begin{aligned}\left\{\hat{\mathbf{X}}_{1,\mathrm{MAP}}, \Delta\hat{\mathbf{X}}_{\mathrm{MAP}}\right\} \in \arg\min_{\mathbf{X}_1, \Delta\mathbf{X}} & \left\|\mathbf{\Lambda}_{\mathrm{LR}}^{-\frac{1}{2}}\left(\mathbf{Y}_{\mathrm{LR}} - \mathbf{X}_1\mathbf{R}\right)\right\|_F^2 \\ & + \left\|\mathbf{\Lambda}_{\mathrm{HR}}^{-\frac{1}{2}}\left(\mathbf{Y}_{\mathrm{HR}} - \mathbf{L}\left(\mathbf{X}_1 + \Delta\mathbf{X}\right)\right)\right\|_F^2 \\ & + \mu\phi_1\left(\mathbf{X}_1\right) + \gamma\phi_2\left(\Delta\mathbf{X}\right)\end{aligned}$$

Key ingredient: ϕ_2

Spatial sparsity of the changes through a group-lasso regularization

$$\begin{aligned}\phi_2\left(\Delta\mathbf{X}\right) &= \|\Delta\mathbf{X}\|_{2,1} \\ &= \sum_{i=1}^{n}\|\Delta\mathbf{x}_i\|_2 = \|\mathbf{e}\|_1\end{aligned}$$

promoting a sparse change image energy vector $\mathbf{e} = \left[\|\Delta\mathbf{x}_1\|_2, \ldots, \|\Delta\mathbf{x}_n\|_2\right]$.

Solution

Robust fusion: alternate minimization algorithm [FDWC17, FDC20]

Data: $\mathbf{Y}_{\mathrm{HR}}, \mathbf{Y}_{\mathrm{LR}}, \mathbf{L}, \mathbf{R}$
Input: $\Delta\mathbf{X}^0$
for $k = 1, \ldots, K$ **do**
 `// Fusion step`
 $\mathbf{X}_1^{(k+1)} = \arg\min_{\mathbf{X}_1} \mathcal{J}(\mathbf{X}_1, \Delta\mathbf{X}^{(k)})$
 `// Correction step`
 $\Delta\mathbf{X}^{(k+1)} = \arg\min_{\Delta\mathbf{X}} \mathcal{J}(\mathbf{X}_1^{(k+1)}, \Delta\mathbf{X})$
end
$\hat{\mathbf{X}}_{1,\mathrm{MAP}} \triangleq \mathbf{X}_1^{(K+1)}$ and $\Delta\hat{\mathbf{X}}_{\mathrm{MAP}} \triangleq \Delta\hat{\mathbf{X}}^{(K+1)}$
Output: $\hat{\mathbf{X}}_{1,\mathrm{MAP}}, \Delta\hat{\mathbf{X}}_{\mathrm{MAP}}$

Characteristics

- Iterative minimization,
- Problem split into 2 simple sub-problems,
- Convergence guarantee.

Optimization w.r.t. $\mathbf{X}_1$
(fixing $\Delta\mathbf{X} = \Delta\mathbf{X}^{(k)}$)

$$\min_{\mathbf{X}_1, \Delta\mathbf{X}} \left\| \mathbf{\Lambda}_{\mathrm{LR}}^{-\frac{1}{2}} \left(\mathbf{Y}_{\mathrm{LR}} - \mathbf{X}_1 \mathbf{R}\right) \right\|_{\mathrm{F}}^2 + \left\| \mathbf{\Lambda}_{\mathrm{HR}}^{-\frac{1}{2}} \left(\mathbf{Y}_{\mathrm{HR}} - \mathbf{L}\left(\mathbf{X}_1 + \Delta\mathbf{X}\right)\right) \right\|_{\mathrm{F}}^2 + \mu \left\|\mathbf{X}_1\right\|_{\mathrm{F}}^2 + \gamma \left\|\Delta\mathbf{X}\right\|_{2,1}$$

Optimization problem

$$\mathbf{X}_1^{(k+1)} = \arg\min_{\mathbf{X}_1} \left\| \mathbf{\Lambda}_{\mathrm{LR}}^{-\frac{1}{2}} \left(\mathbf{Y}_{\mathrm{LR}} - \mathbf{X}_1 \mathbf{R}\right) \right\|_{\mathrm{F}}^2 + \left\| \mathbf{\Lambda}_{\mathrm{HR}}^{-\frac{1}{2}} \left(\mathbf{Y}_{\mathrm{HR}} - \mathbf{L}\left(\mathbf{X}_1 + \Delta\mathbf{X}^{(k)}\right)\right) \right\|_{\mathrm{F}}^2 + \mu \left\|\mathbf{X}_1\right\|_{\mathrm{F}}^2$$

rewritten as

$$\mathbf{X}_1^{(k+1)} = \arg\min_{\mathbf{X}_1} \left\| \mathbf{\Lambda}_{\mathrm{LR}}^{-\frac{1}{2}} \left(\mathbf{Y}_{\mathrm{LR}} - \mathbf{X}_1 \mathbf{R}\right) \right\|_{\mathrm{F}}^2 + \left\| \mathbf{\Lambda}_{\mathrm{HR}}^{-\frac{1}{2}} \left(\widetilde{\mathbf{Y}}_{\mathrm{HR}}^{(k)} - \mathbf{L}\mathbf{X}_1\right) \right\|_{\mathrm{F}}^2 + \mu \left\|\mathbf{X}_1\right\|_{\mathrm{F}}^2$$

with

- $\widetilde{\mathbf{Y}}_{\mathrm{HR}}^{k} = \mathbf{Y}_{\mathrm{HR}} - \mathbf{L}\Delta\mathbf{X}^{(k)}$: pseudo-observed image at t_1.
- Equivalent to an image fusion problem (single latent image estimation $\mathbf{X}_1$).
- Two quadratic data-fitting terms + Thikonov regularization
  - $\rightarrow$ fast and explicit solution based on solving a Sylvester equation.

Optimization w.r.t. $\mathbf{X}_1$
(fixing $\Delta\mathbf{X} = \Delta\mathbf{X}^{(k)}$)

$$\min_{\mathbf{X}_1,\Delta\mathbf{X}} \left\|\boldsymbol{\Lambda}_{\mathrm{LR}}^{-\frac{1}{2}}\left(\mathbf{Y}_{\mathrm{LR}} - \mathbf{X}_1\mathbf{R}\right)\right\|_{\mathrm{F}}^2 + \left\|\boldsymbol{\Lambda}_{\mathrm{HR}}^{-\frac{1}{2}}\left(\mathbf{Y}_{\mathrm{HR}} - \mathbf{L}\left(\mathbf{X}_1 + \Delta\mathbf{X}\right)\right)\right\|_{\mathrm{F}}^2 + \mu\left\|\mathbf{X}_1\right\|_{\mathrm{F}}^2 + \gamma\left\|\Delta\mathbf{X}\right\|_{2,1}$$

Optimization problem

$$\mathbf{X}_1^{(k+1)} = \arg\min_{\mathbf{X}_1} \left\|\boldsymbol{\Lambda}_{\mathrm{LR}}^{-\frac{1}{2}}\left(\mathbf{Y}_{\mathrm{LR}} - \mathbf{X}_1\mathbf{R}\right)\right\|_{\mathrm{F}}^2 + \left\|\boldsymbol{\Lambda}_{\mathrm{HR}}^{-\frac{1}{2}}\left(\mathbf{Y}_{\mathrm{HR}} - \mathbf{L}\left(\mathbf{X}_1 + \Delta\mathbf{X}^{(k)}\right)\right)\right\|_{\mathrm{F}}^2 + \mu\left\|\mathbf{X}_1\right\|_{\mathrm{F}}^2$$

rewritten as

$$\mathbf{X}_1^{(k+1)} = \arg\min_{\mathbf{X}_1} \left\|\boldsymbol{\Lambda}_{\mathrm{LR}}^{-\frac{1}{2}}\left(\mathbf{Y}_{\mathrm{LR}} - \mathbf{X}_1\mathbf{R}\right)\right\|_{\mathrm{F}}^2 + \left\|\boldsymbol{\Lambda}_{\mathrm{HR}}^{-\frac{1}{2}}\left(\widetilde{\mathbf{Y}}_{\mathrm{HR}}^{(k)} - \mathbf{L}\mathbf{X}_1\right)\right\|_{\mathrm{F}}^2 + \mu\left\|\mathbf{X}_1\right\|_{\mathrm{F}}^2$$

with

- $\widetilde{\mathbf{Y}}_{\mathrm{HR}}^{k} = \mathbf{Y}_{\mathrm{HR}} - \mathbf{L}\Delta\mathbf{X}^{(k)}$: pseudo-observed image at t_1.
- Equivalent to an image fusion problem (single latent image estimation $\mathbf{X}_1$).
- Two quadratic data-fitting terms + Thikonov regularization
  - $\rightarrow$ fast and explicit solution based on solving a Sylvester equation.

Optimization w.r.t. $\mathbf{X}_1$

(fixing $\Delta\mathbf{X} = \Delta\mathbf{X}^{(k)}$)

$$\min_{\mathbf{X}_1, \Delta\mathbf{X}} \left\| \boldsymbol{\Lambda}_{\mathrm{LR}}^{-\frac{1}{2}} \left(\mathbf{Y}_{\mathrm{LR}} - \mathbf{X}_1 \mathbf{R}\right) \right\|_{\mathrm{F}}^2 + \left\| \boldsymbol{\Lambda}_{\mathrm{HR}}^{-\frac{1}{2}} \left(\mathbf{Y}_{\mathrm{HR}} - \mathbf{L}\left(\mathbf{X}_1 + \Delta\mathbf{X}\right)\right) \right\|_{\mathrm{F}}^2 + \mu \left\|\mathbf{X}_1\right\|_{\mathrm{F}}^2 + \gamma \left\|\Delta\mathbf{X}\right\|_{2,1}$$

Optimization problem

$$\mathbf{X}_1^{(k+1)} = \arg\min_{\mathbf{X}_1} \left\| \boldsymbol{\Lambda}_{\mathrm{LR}}^{-\frac{1}{2}} \left(\mathbf{Y}_{\mathrm{LR}} - \mathbf{X}_1 \mathbf{R}\right) \right\|_{\mathrm{F}}^2 + \left\| \boldsymbol{\Lambda}_{\mathrm{HR}}^{-\frac{1}{2}} \left(\mathbf{Y}_{\mathrm{HR}} - \mathbf{L}\left(\mathbf{X}_1 + \Delta\mathbf{X}^{(k)}\right)\right) \right\|_{\mathrm{F}}^2 + \mu \left\|\mathbf{X}_1\right\|_{\mathrm{F}}^2$$

rewritten as

$$\mathbf{X}_1^{(k+1)} = \arg\min_{\mathbf{X}_1} \left\| \boldsymbol{\Lambda}_{\mathrm{LR}}^{-\frac{1}{2}} \left(\mathbf{Y}_{\mathrm{LR}} - \mathbf{X}_1 \mathbf{R}\right) \right\|_{\mathrm{F}}^2 + \left\| \boldsymbol{\Lambda}_{\mathrm{HR}}^{-\frac{1}{2}} \left(\widetilde{\mathbf{Y}}_{\mathrm{HR}}^{(k)} - \mathbf{L}\mathbf{X}_1\right) \right\|_{\mathrm{F}}^2 + \mu \left\|\mathbf{X}_1\right\|_{\mathrm{F}}^2$$

with

- $\widetilde{\mathbf{Y}}_{\mathrm{HR}}^{k} = \mathbf{Y}_{\mathrm{HR}} - \mathbf{L}\Delta\mathbf{X}^{(k)}$: pseudo-observed image at t_1.
- Equivalent to an image fusion problem (single latent image estimation $\mathbf{X}_1$).
- Two quadratic data-fitting terms + Thikonov regularization

  $\rightarrow$ fast and explicit solution based on solving a Sylvester equation.

Optimization w.r.t. $\Delta\mathbf{X}$
(fixing $\mathbf{X}_1 = \mathbf{X}_1^{(k)}$)

$$\min_{\mathbf{X}_1,\Delta\mathbf{X}} \left\|\mathbf{\Lambda}_{\mathrm{LR}}^{-\frac{1}{2}}\left(\mathbf{Y}_{\mathrm{LR}} - \mathbf{X}_1\mathbf{R}\right)\right\|_{\mathrm{F}}^2 + \left\|\mathbf{\Lambda}_{\mathrm{HR}}^{-\frac{1}{2}}\left(\mathbf{Y}_{\mathrm{HR}} - \mathbf{L}\left(\mathbf{X}_1 + \Delta\mathbf{X}\right)\right)\right\|_{\mathrm{F}}^2 + \mu\left\|\mathbf{X}_1\right\|_{\mathrm{F}}^2 + \gamma\left\|\Delta\mathbf{X}\right\|_{2,1}$$

Optimization problem

$$\Delta\mathbf{X}^{(k+1)} = \arg\min_{\Delta\mathbf{X}} \left\|\mathbf{\Lambda}_{\mathrm{HR}}^{-\frac{1}{2}}\left(\Delta\mathbf{Y}_{\mathrm{HR}} - \mathbf{L}\left(\mathbf{X}_1^k + \Delta\mathbf{X}\right)\right)\right\|_{\mathrm{F}}^2 + \gamma\left\|\Delta\mathbf{X}\right\|_{2,1}$$

rewritten as

$$\Delta\mathbf{X}^{(k+1)} = \arg\min_{\Delta\mathbf{X}} \left\|\mathbf{\Lambda}_{\mathrm{HR}}^{-\frac{1}{2}}\left(\Delta\widetilde{\mathbf{Y}}_{\mathrm{HR}}^k - \mathbf{L}\Delta\mathbf{X}\right)\right\|_{\mathrm{F}}^2 + \gamma\left\|\Delta\mathbf{X}\right\|_{2,1}$$

with

- $\Delta\widetilde{\mathbf{Y}}_{\mathrm{HR}}^k = \mathbf{Y}_{\mathrm{HR}} - \mathbf{L}\mathbf{X}_1^k$: predicted change image at t_2.
- Equivalent to a spectral debluring problem.
- Convex data-fitting term and regularization, non-smooth regularization
  $\rightarrow$ solution using proximal algorithms (i.e. forward-backward).

Optimization w.r.t. $\Delta\mathbf{X}$
(fixing $\mathbf{X}_1 = \mathbf{X}_1^{(k)}$)

$$\min_{\mathbf{X}_1, \Delta\mathbf{X}} \left\| \boldsymbol{\Lambda}_{\mathrm{LR}}^{-\frac{1}{2}} \left(\mathbf{Y}_{\mathrm{LR}} - \mathbf{X}_1 \mathbf{R} \right) \right\|_{\mathrm{F}}^2 + \left\| \boldsymbol{\Lambda}_{\mathrm{HR}}^{-\frac{1}{2}} \left(\mathbf{Y}_{\mathrm{HR}} - \mathbf{L} \left(\mathbf{X}_1 + \Delta\mathbf{X} \right) \right) \right\|_{\mathrm{F}}^2 + \mu \left\| \mathbf{X}_1 \right\|_{\mathrm{F}}^2 + \gamma \left\| \Delta\mathbf{X} \right\|_{2,1}$$

Optimization problem

$$\Delta\mathbf{X}^{(k+1)} = \arg\min_{\Delta\mathbf{X}} \left\| \boldsymbol{\Lambda}_{\mathrm{HR}}^{-\frac{1}{2}} \left(\Delta\mathbf{Y}_{\mathrm{HR}} - \mathbf{L} \left(\mathbf{X}_1^k + \Delta\mathbf{X} \right) \right) \right\|_{\mathrm{F}}^2 + \gamma \left\| \Delta\mathbf{X} \right\|_{2,1}$$

rewritten as

$$\Delta\mathbf{X}^{(k+1)} = \arg\min_{\Delta\mathbf{X}} \left\| \boldsymbol{\Lambda}_{\mathrm{HR}}^{-\frac{1}{2}} \left(\Delta\widetilde{\mathbf{Y}}_{\mathrm{HR}}^k - \mathbf{L}\Delta\mathbf{X} \right) \right\|_{\mathrm{F}}^2 + \gamma \left\| \Delta\mathbf{X} \right\|_{2,1}$$

with

- $\Delta\widetilde{\mathbf{Y}}_{\mathrm{HR}}^k = \mathbf{Y}_{\mathrm{HR}} - \mathbf{L}\mathbf{X}_1^k$: predicted change image at t_2.
- Equivalent to a spectral debluring problem.
- Convex data-fitting term and regularization, non-smooth regularization
  $\rightarrow$ solution using proximal algorithms (i.e. forward-backward).

Optimization w.r.t. $\Delta\mathbf{X}$
(fixing $\mathbf{X}_1 = \mathbf{X}_1^{(k)}$)

$$\min_{\mathbf{X}_1, \Delta\mathbf{X}} \left\| \mathbf{\Lambda}_{\mathrm{LR}}^{-\frac{1}{2}} \left(\mathbf{Y}_{\mathrm{LR}} - \mathbf{X}_1 \mathbf{R} \right) \right\|_{\mathrm{F}}^2 + \left\| \mathbf{\Lambda}_{\mathrm{HR}}^{-\frac{1}{2}} \left(\mathbf{Y}_{\mathrm{HR}} - \mathbf{L}\left(\mathbf{X}_1 + \Delta\mathbf{X} \right) \right) \right\|_{\mathrm{F}}^2 + \mu \left\| \mathbf{X}_1 \right\|_{\mathrm{F}}^2 + \gamma \left\| \Delta\mathbf{X} \right\|_{2,1}$$

Optimization problem

$$\Delta\mathbf{X}^{(k+1)} = \arg\min_{\Delta\mathbf{X}} \left\| \mathbf{\Lambda}_{\mathrm{HR}}^{-\frac{1}{2}} \left(\Delta\mathbf{Y}_{\mathrm{HR}} - \mathbf{L}\left(\mathbf{X}_1^k + \Delta\mathbf{X} \right) \right) \right\|_{\mathrm{F}}^2 + \gamma \left\| \Delta\mathbf{X} \right\|_{2,1}$$

rewritten as

$$\Delta\mathbf{X}^{(k+1)} = \arg\min_{\Delta\mathbf{X}} \left\| \mathbf{\Lambda}_{\mathrm{HR}}^{-\frac{1}{2}} \left(\Delta\widetilde{\mathbf{Y}}_{\mathrm{HR}}^k - \mathbf{L}\Delta\mathbf{X} \right) \right\|_{\mathrm{F}}^2 + \gamma \left\| \Delta\mathbf{X} \right\|_{2,1}$$

with

- $\Delta\widetilde{\mathbf{Y}}_{\mathrm{HR}}^k = \mathbf{Y}_{\mathrm{HR}} - \mathbf{L}\mathbf{X}_1^k$: predicted change image at t_2.
- Equivalent to a spectral debluring problem.
- Convex data-fitting term and regularization, non-smooth regularization
  $\rightarrow$ solution using proximal algorithms (i.e. forward-backward).

Experiments on synthetic images

Detection performance

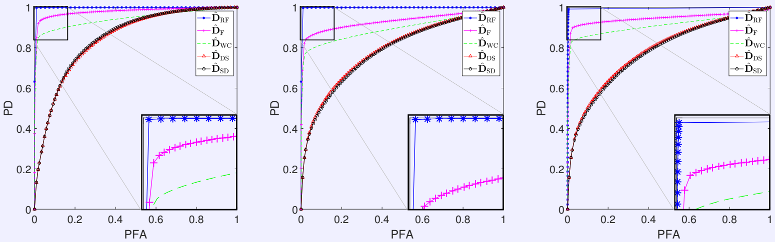

(a) Situation 1: HR-MS/LR-HS

(b) Situation 2: HR-PAN/LR-HS

(c) Situation 3: HR-PAN/LR-MS

Table: Situations 1 , 2 & 3: quantitative detection performance (AUC and distance).

		$\hat{\mathbf{D}}_{\mathrm{RF}}$	$\hat{\mathbf{D}}_{\mathrm{F}}$	$\hat{\mathbf{D}}_{\mathrm{WC}}$	$\hat{\mathbf{D}}_{\mathrm{DS}}$	$\hat{\mathbf{D}}_{\mathrm{SD}}$
Situation 1	AUC	**0.997469**	0.981039	0.941408	0.843685	0.847518
	Dist.	**0.990299**	0.951995	0.887789	0.766677	0.771277
Situation 2	AUC	**0.997418**	0.931047	0.89517	0.790859	0.785019
	Dist.	**0.990299**	0.883488	0.833783	0.718072	0.712771
Situation 3	AUC	**0.994929**	0.94522	0.911311	0.786255	0.779522
	Dist.	**0.991699**	0.915992	0.864686	0.713471	0.706871

Experiments on real images
Data description

Observed image at t_1 (04/15/2015):

- Local: Lake-Tahoe (CA) USA.
- Sensor: Landsat 8.
- Image size: 175 $\times$ 180 pixels.
- Spatial resolution: 30m per pixel.
- Spectral resolution: 3 spectral bands (MS) in RBG visible spectrum .

Observed image at t_2 (09/22/2015):

- Local: Lake-Tahoe (CA) USA.
- Sensor: Landsat 8.
- Image size: 350 $\times$ 360 pixels.
- Spatial resolution: 15m per pixel.
- Spectral resolution: PAN in RBG visible spectrum .

Preprocessing:

- Manual alignment.

Compared Methods:

- Robust Fusion approach ($\hat{\mathbf{D}}_{\mathrm{RF}}$).
- Fusion approach ($\hat{\mathbf{D}}_{\mathrm{F}}$) .
- Worst-case approach ($\hat{\mathbf{D}}_{\mathrm{WC}}$).

Experiments on real images
Visual results

(a) $\mathbf{Y}_1$ (b) $\mathbf{Y}_2$ (c) $\hat{\mathbf{D}}_{\mathrm{RF}}$ (d) $\hat{\mathbf{D}}_{\mathrm{F}}$ (e) $\hat{\mathbf{D}}_{\mathrm{WC}}$

(f) zoomed $\mathbf{Y}_1$ (g) zoomed $\mathbf{Y}_2$ (h) zoomed $\hat{\mathbf{D}}_{\mathrm{RF}}$ (i) zoomed $\hat{\mathbf{D}}_{\mathrm{F}}$ (j) zoomed $\hat{\mathbf{D}}_{\mathrm{WC}}$

Scenario $\mathcal{S}_4$: (a) LR-MS observed image $\mathbf{Y}_{\mathrm{LR}}$, (b) HR-PAN observed image $\mathbf{Y}_{\mathrm{HR}}$, (e) change mask $\hat{\mathbf{D}}_{\mathrm{WC}}$ estimated by the WC approach, (d) change mask $\hat{\mathbf{D}}_{\mathrm{F}}$ estimated by the fusion approach and (c) change mask $\hat{\mathbf{D}}_{\mathrm{RF}}$ estimated by the proposed approach. From (f) to (h): zoomed versions of the regions delineated in red in (a)–(c).

Outline

Introduction

Multi-band optical image fusion
- Problem statement
- Fast fusion solving a Sylvester equation
- Experiments

Multi-band optical image change detection
- Fusion approach
- Robust Fusion approach

Conclusions

Fusion

- fusion of multi-band images formulated as a linear inverse problem
- spectral regularization: constraining the estimation in a lower-dimensional space
- spatial regularizations:
  - Gaussian prior
  - dictionary-based sparse prior
  - ...
- explicit solution under generalized Thinonov regularizations, which can be embedded into iterative algorithms
  - for more complex priors
  - when estimating jointly other parameters (noise variance, spectral response,...)

- assumes spectrally-invariant spatial blurs... not valid for astrophysical data
  $\rightarrow$ see [GOBD20] and [GOB$^+$20]

- fusion as a convenient framework to address change detection problems

Fusion

- fusion of multi-band images formulated as a linear inverse problem
- spectral regularization: constraining the estimation in a lower-dimensional space
- spatial regularizations:
  - Gaussian prior
  - dictionary-based sparse prior
  - ...
- explicit solution under generalized Thinonov regularizations, which can be embedded into iterative algorithms
  - for more complex priors
  - when estimating jointly other parameters (noise variance, spectral response,...)

- assumes spectrally-invariant spatial blurs... not valid for astrophysical data
  $\rightarrow$ see [GOBD20] and [GOB$^+$20]

- fusion as a convenient framework to address change detection problems

Fusion

- fusion of multi-band images formulated as a linear inverse problem
- spectral regularization: constraining the estimation in a lower-dimensional space
- spatial regularizations:
  - Gaussian prior
  - dictionary-based sparse prior
  - ...
- explicit solution under generalized Thinonov regularizations, which can be embedded into iterative algorithms
  - for more complex priors
  - when estimating jointly other parameters (noise variance, spectral response,...)

- assumes spectrally-invariant spatial blurs... not valid for astrophysical data
  $\rightarrow$ see [GOBD20] and [GOB^{+}20]

- fusion as a convenient framework to address change detection problems

Change detection

Fusion approach

- unsupervised CD between optical images of different spatial/spectral resolutions
- assumes prior knowledge on the forward model (degradations)
- steps tailored by the end-user
- provides 2 CD maps of different resolutions

Robust fusion approach

- unsupervised CD between optical images of different spatial/spectral resolutions
- assumes prior knowledge on the forward model (degradations)
- estimates high resolution latent images and CD images
- provides 1 CD map of high spatial and spectral resolutions

For images of different modalities (e.g., optical and SAR)

- no forward model available
- no physically interpretable latent space
- latent space identified by data-driven methods, e.g., dictionary learning [FDC+19]

Change detection

Fusion approach

- unsupervised CD between optical images of different spatial/spectral resolutions
- assumes prior knowledge on the forward model (degradations)
- steps tailored by the end-user
- provides 2 CD maps of different resolutions

Robust fusion approach

- unsupervised CD between optical images of different spatial/spectral resolutions
- assumes prior knowledge on the forward model (degradations)
- estimates high resolution latent images and CD images
- provides 1 CD map of high spatial and spectral resolutions

For images of different modalities (e.g., optical and SAR)

- no forward model available
- no physically interpretable latent space
- latent space identified by data-driven methods, e.g., dictionary learning [FDC+19]

References I

Francesca Bovolo and Lorenzo Bruzzone.
A Theoretical Framework for Unsupervised Change Detection Based on Change Vector Analysis in the Polar Domain.
IEEE Trans. Geosci. Remote Sens., 45(1):218–236, 2007.

V. Ferraris, N. Dobigeon, Y. Cruz Cavalcanti, Th. Oberlin, and M. Chabert.
Coupled dictionary learning for unsupervised change detection between multimodal remote sensing images.
Computer Vision and Image Understanding, 189(102817), Dec. 2019.

V. Ferraris, N. Dobigeon, and M. Chabert.
Robust fusion algorithms for unsupervised change detection between multi-band optical images – A comprehensive case study.
Information Fusion, 64:293–317, Dec. 2020.

V. Ferraris, N. Dobigeon, Q. Wei, and M. Chabert.
Robust fusion of multi-band images with different spatial and spectral resolutions for change detection.
IEEE Trans. Computational Imaging, 3(2):175–186, April 2017.

V. Ferraris, N. Dobigeon, Q. Wei, and M. Chabert.
Detecting changes between optical images of different spatial and spectral resolutions: a fusion-based approach.
IEEE Trans. Geoscience and Remote Sensing, 56(3):1566–1578, March 2018.

References II

V. Ferraris, N. Yokoya, N. Dobigeon, and M. Chabert.
A comparative study of fusion-based change detection methods for multi-band images with different spectral and spatial resolutions.
In *Proc. IEEE Int. Geosci. Remote Sens. Symp. (IGARSS)*, pages 5021–5024, Valencia, Spain, July 2018.

C. Guilloteau, Th. Oberlin, O. Berné, É. Habart, and N. Dobigeon.
Simulated JWST datasets for multispectral and hyperspectral image fusion.
The Astronomical Journal, 160(1):28, Jun. 2020.

C. Guilloteau, Th. Oberlin, O. Berné, and N. Dobigeon.
Hyperspectral and multispectral image fusion under spectrally varying spatial blurs – application to high dimensional infrared astronomical imaging.
IEEE Trans. Computational Imaging, 6:1362–1374, Sept. 2020.

Maoguo Gong, Puzhao Zhang, Linzhi Su, and Jia Liu.
Coupled Dictionary Learning for Change Detection From Multisource Data.
IEEE Trans. Geosci. Remote Sens., 54(12):7077–7091, 2016.

M. N. Klaric, B. C. Claywell, G. J. Scott, N. J. Hudson, O. Sjahputera, Yonghong Li, S. T. Barratt, J. M. Keller, and C. H. Davis.
GeoCDX: An Automated Change Detection and Exploitation System for High-Resolution Satellite Imagery.
IEEE Trans. Geosci. Remote Sens., 51(4):2067–2086, 2013.

References III

L. Loncan, J. M. Bioucas-Dias, X. Briottet, J. Chanussot, N. Dobigeon, S. Fabre, W. Liao, G. Licciardi, M. Simoes, J-Y. Tourneret, M. Veganzones, G. Vivone, Q. Wei, and N. Yokoya.
Hyperspectral pansharpening: a review.
IEEE Geosci. Remote Sens. Mag., 3(3):27–46, Sept. 2015.

Laetitia Loncan, Luis B. de Almeida, Jose M. Bioucas-Dias, Xavier Briottet, Jocelyn Chanussot, Nicolas Dobigeon, Sophie Fabre, Wenzhi Liao, Giorgio A. Licciardi, Miguel Simoes, Jean-Yves Tourneret, Miguel Angel Veganzones, Gemine Vivone, Qi Wei, and Naoto Yokoya.
Hyperspectral Pansharpening: A Review.
IEEE Geosci. Remote Sens. Mag., 3(3):27–46, 2015.

Union of Concerned Scientists.
Union of concerned scientists satellite database.
`https://www.ucsusa.org/nuclear-weapons/space-weapons/satellite-database#.WigLykqnFPY`, 2017.

Jorge Prendes, Marie Chabert, Frédéric Pascal, Alain Giros, and Jean-Yves Tourneret.
Change detection for optical and radar images using a Bayesian nonparametric model coupled with a Markov random field.
In *Proc. IEEE Int. Conf. Acoust., Speech and Signal Process. (ICASSP)*, pages 1513–1517. IEEE, 2015.

M. Simões, J. Bioucas Dias, L. Almeida, and J. Chanussot.
A convex formulation for hyperspectral image superresolution via subspace-based regularization.
IEEE Trans. Geosci. Remote Sens., 53(6):3373–3388, 2015.

References IV

Q. Wei, J. M. Bioucas Dias, N. Dobigeon, and J.-Y. Tourneret.
Hyperspectral and multispectral image fusion based on a sparse representation.
IEEE Trans. Geosci. Remote Sens., 53(7):3658–3668, 2015.

Q. Wei, N. Dobigeon, and J.-Y. Tourneret.
Fast fusion of multi-band images based on solving a Sylvester equation.
IEEE Trans. Image Processing, 24(11):4109–4121, Nov. 2015.

Qi Wei, Nicolas Dobigeon, and Jean-Yves Tourneret.
Bayesian fusion of multi-band images.
IEEE J. Sel. Topics Signal Processing, (6):1117–1127, 9 2015.

Qi Wei, Nicolas Dobigeon, and Jean-Yves Tourneret.
Bayesian fusion of multispectral and hyperspectral images using a block coordinate descent method.
In *Proc. IEEE GRSS Workshop Hyperspectral Image SIgnal Process.: Evolution in Remote Sens. (WHISPERS)*, Tokyo, Japan, June 2015.

Q. Wei, N. Dobigeon, J.-Y. Tourneret, J. M. Bioucas-Dias, and S. Godsill.
R-FUSE: Robust fast fusion of multi-band images based on solving a Sylvester equation.
IEEE Signal Processing Letters, 23(11):1632–1636, Nov. 2016.

Lucien Wald, Thierry Ranchin, and Marc Mangolini.
Fusion of satellite images of different spatial resolutions: Assessing the quality of resulting images.
Photogrammetric engineering and remote sensing, 63(6):691–699, 1997.

References V

N. Zhao, Q. Wei, A. Basarab, N. Dobigeon, D. Kouamé, and J.-Y. Tourneret.
Fast single image super-resolution using a new analytical solution for $\ell_2 - \ell_2$ problems.
IEEE Trans. Image Processing, 25(8):3683–3697, Aug. 2016.

Multi-band optical imaging

From fusion to change detection

Nicolas Dobigeon
Joint work with Q. Wei, V. Ferraris, J.-Y. Tourneret and M. Chabert

University of Toulouse, IRIT/INP-ENSEEIHT
Institut Universitaire de France (IUF)
Artificial and Natural Intelligence Toulouse Institute (ANITI)
http://dobigeon.perso.enseeiht.fr

ORASIS 2021, Lac de St-Ferréol